AN ABSTRACT OF THE THESIS OF

Elizabeth Lev Brunner for the degree of Master of Science in Ocean, Earth and Atmospheric Sciences presented on October 28, 2013

Title: Insights from Stable Isotope Dynamics into the Sensitivity of Larval Pacific Oysters to Ocean Acidification

Abstract approved: _____

George G. Waldbusser

Larvae of the Pacific Oyster, *Crassostrea gigas*, at Whiskey Creek Shellfish Hatchery (WCH) in Netarts Bay, Oregon, are negatively impacted by high-CO_2 water and exposure during the initial shell formation period appears to be particularly damaging. To investigate the mechanism of this early susceptibility, several cohorts of larvae at WCH were monitored for stable isotope incorporation and biochemical composition: one in May 2011 and two in August 2011. The observations presented here focus on the isotopic shifts associated with initiation and rate of feeding, and the catabolism of C-rich (lipid) and N-rich (protein) pools. Persistent ontological patterns in bulk composition among the cohorts suggest that the creation of the initial shell is energetically expensive, and that the major energetic source during this period is maternally-derived egg lipids. The May cohort did not isotopically reflect their food source as rapidly as the August cohorts, indicating slower feeding, higher metabolic demand or lower maternal energy investments. All cohorts turned over organic carbon faster than organic nitrogen.

Shell carbon isotopes of all cohorts show a decreasing dependence on ambient dissolved inorganic carbon (DIC) carbon with time and subtle differences in this trend between the May and August cohorts are explored. Patterns in shell $\delta^{13}C$ suggest greater exposure to ambient conditions during initial shell development, which could be an important process linking ambient carbonate chemistry and larval susceptibility. Scanning electron microscopy (SEM) images are used to document the initial shell formation. Kinetic isotope fractionation, dissolved organic matter (DOM) utilization, and

the dissolvability of shell microstructures are also briefly considered in the context of larval susceptibility.

Insights from Stable Isotope Dynamics into the Sensitivity of Larval Pacific Oysters to Ocean Acidification

by
Elizabeth Lev Brunner

A THESIS

submitted to

Oregon State University

in partial fulfillment of
the requirements for the
degree of

Master of Science

Presented October 28, 2013
Commencement June 2014

Master of Science thesis of Elizabeth Lev Brunner presented on October 28th, 2013

APPROVED:

_____
Major Professor, representing Ocean, Earth and Atmospheric Sciences

_____
Dean of the College of Earth, Ocean and Atmospheric Sciences

_____
Dean of the Graduate School

I understand that my thesis will become part of the permanent collection of Oregon State University libraries. My signature below authorizes release of my thesis to any reader upon request.

_____
Elizabeth Lev Brunner, Author

ACKNOWLEDGEMENTS

Elias Hannon, Olivia Miller, Elsa Gustavson, Alden Gray, and Katelyn Banta among others. In particular, I would like to extend an extra-special thank you to my brilliant and kind office-mate Iria Gimenez who transcends many of the categories of supporter I just defined. Iria, I seriously couldn't have done all of this without your support, guidance, and friendship. You can count on me to throw you one heck of a party when you finish your PhD.

And finally, thanks to Timothy Hemphill, who moved all the way to Corvallis, from Washington, DC just for little old me. Thank you. Thank you so much for being an amazing part of my life, and believing in me and my abilities, even when I didn't. Thank you for all that you've put up with, and for encouraging me to make the hard and scary decision to step off the speeding train of academia and re-evaluate what I want to do with my time. Thank you for being an amazing example of what it means to follow your dreams.

TABLE OF CONTENTS

LIST OF TABLES

LIST OF FIGURES

LIST OF APPENDIX TABLES

LIST OF APPENDIX FIGURES

INTRODUCTION

Eastern-boundary upwelling ecosystems like the California Current Ecosystem have been identified as "hotspots" for ocean acidification (OA) impacts (Feely et al. 2008, Gruber 2011, Hauri et al. 2013a, Harris et al. 2013). The California Current System, which supplies water to North American West Coast estuaries (Hickey & Banas 2003), is projected to become more frequently, more extensively, and more severely undersaturated with respect to aragonite in coming decades (Hauri et al. 2013b). Estuarine carbonate chemistry is highly variable on seasonal to hourly timescales (Borges et al. 2006, Hunt et al. 2011, Hofmann et al. 2011, Evans et al. 2013) but an increasing CO_2 baseline means that the periods of high (>>1) saturation state will be increasingly scarce (Hauri et al. 2013b). The timing of these undersaturation events relative to ecological processes (i.e., reproduction, critical life-history periods) will determine the magnitude and type of ecological impacts (Waldbusser & Salisbury 2014). The impacts of ocean acidification on estuarine organisms are just beginning to be observed (e.g., Barton et al. 2012), but OA is projected to increasingly impact organisms and ecosystems in coming decades. Indeed, the combined impacts of ocean acidification, ocean warming, sea-level rise and changes in ocean productivity will keep ocean ecosystems in a state of continuous change for the next 100,000 years (Gruber 2011, Norris et al. 2013)

Impacts of high-CO_2-water on *C. gigas* larvae have already been observed in shellfish hatcheries along the West Coast (Barton et al. 2012). In 2012, the Washington State Blue Ribbon Panel on Ocean Acidification identified "laboratory studies to assess the direct effects of ocean acidification, alone and in combination with other stressors, on local species and ecosystems" as a key early action for responding to OA in Washington State (Adelsman and Binder, 2012). Bivalve larvae appear to be most sensitive to ambient carbonate chemistry in the two days following fertilization (Kurihara 2008, Barton et al. 2012, Gobler & Talmage 2013), while they are forming the initial, or "D-hinge" shell. In a series of experiments on *Argopecten irradians*, White et al. (2013) found differential sensitivity to exposure to high PCO_2 water in different parts of the larval period, beginning 0-2 hours after fertilization. Although the fundamental mechanism of this sensitivity is a subject of great interest (Waldbusser et al., 2013), and

the subject of several recent reviews (Kroeker et al. 2010, Parker et al. 2013, Gazeau et al. 2013), there are aspects that have not been fully explored. One reason for this is that effects of sub-lethal OA stress do not always manifest themselves immediately in growth or survival so many commonly-used metrics of success (e.g., length at D-hinge, co-incident survival) cannot fully capture the impacts. For example, the effects described by Barton et al. (2012), were seen more than a week after exposure in early life — a kind-of "carry over" effect similar to those observed by (Hettinger et al. 2012, 2013) for *Ostrea lurida* and by Gobler and Talmage (2013) in *Mercenaria mercenaria*.

Early ocean acidification studies tested the response of estuarine organisms to elevated PCO_2 by bubbling seawater with different concentrations of CO_2 gas, – and found responses of marine bivalves that ranged from negative to neutral (Kurihara et al., 2008; Ries et al., 2009; Talmage and Gobler, 2009). These experiments were important in identifying the first order responses, but oyster larvae live in dynamic estuarine environments where they are acted on by biotic and abiotic factors besides acidification (Kennedy 1996). Further research has shown that, as with other physiological stressors, OA impacts can be mediated by the presence/absence of other stressors such as temperature (Waldbusser et al., 2011, Kroeker et al. 2013) and food availability (Melzner et al. 2011) and is variable among life history stages (Waldbusser et al., 2010, Barton et al. 2012, White et al. 2013). It has also long been recognized that broodstock quality is important for determining larval success (Gallager & Mann 1986, Gallager et al. 1986).

Most bivalves mineralize shell orders of magnitude more rapidly than would proceed abiotically in supersaturated seawater. They employ two main energy-demanding processes to do so: the synthesis of organic matrix macromolecules that provide nucleation sites and catalyze the precipitation process (Marin et al. 2008); and the alkalization of the calcifying fluid via proton pumping (McConnaughey and Gillikin, 2008, Ries, 2011). Larval oysters precipitate aragonite (a relatively soluble polymorph of calcium carbonate) which is a commonly-cited rationale for predicting them to be losers in a high CO_2 world. However, thermodynamics cannot explain differential sensitivity within life-history stages with the same mineral polymorph (Waldbusser et al. 2010), nor patterns found across taxa (Ries 2011a). Some studies suggest larval oyster shell is

initiated as the even more unstable amorphous calcium carbonate (ACC) (e.g., Weiss et al. 2002), while others have found no evidence of ACC in the early larval shell (Kudo et al. 2010, Yokoo et al. 2011). Regardless of the polymorph, bivalve larvae create their initial shell (Prodissoconch I) even faster than later (Prodissoconch II) larval shell material (Maeda-Martinez 1987, Waldbusser et al. 2013). Waldbusser et al., (2013) invoked kinetics to explain how the energetic demand of the initial shell precipitation increases exponentially as the ambient water approaches under-saturation, particularly at the rapid calcification rates of this early stage. During the initial shell formation period, he larvae are less able to exert biological control over the calcification process, and the high energetic demand required to complete the initial shell under acidified conditions can result in a lower scope for growth, ultimately putting the larvae into an energetic deficit from which they do not appear to be able to recover. The equation used to describe this kinetic constraint is

$$r = k(\Omega - 1)^n$$

Where r is the mineral precipitation rate, k is the rate constant, Ω is the saturation state of the surrounding seawater with respect to the given mineral, and n is the reaction order constant.

Estuarine organisms will not experience the relatively slow and steady rise in oceanic PCO_2 that is projected for the open-ocean (Waldbusser et al. 2011, Kelly et al. 2011, McElhany & Busch 2013, Waldbusser & Salisbury 2014). Some productive estuarine environments span nearly the entire range of EPOCA-recommended PCO_2 treatments for ocean acidification in just one day (Borges, 2005, Dai et al., 2009, Barry et al. 2010). My thesis builds upon the ideas developed in Waldbusser et al., (2013) and documents the biochemical and energetic changes occurring in early life, by taking advantage of the "natural laboratory" provided by Whiskey Creek Shellfish Hatchery. One distinctive aspect of this study and Waldbusser et al., (2013) is the use of stable isotopes, which have long been used to track the movement of C, N and O in ecological systems and organisms (e.g., DeNiro & Epstein 1978). The cohort-tracking experiments

presented here focus on the isotopic shifts associated with initiation of feeding and our ability to quantify the catabolism and assimilation of C-rich (lipid) and N-rich (protein) compounds. By following multiple hatchery-grown cohorts of larvae, I hope to document fundamental processes in larval shell development and explore the relationship between energetic status and larval success, in order to build our fundamental understanding of the mechanisms of susceptibility of larval bivalves to OA.

METHODS

Setting and Experimental Design

I followed three cohorts of approximately 400 million *Crassostrea gigas* larvae from fertilization through metamorphosis at Whiskey Creek Hatchery (WCH) in Netarts, Oregon: one cohort in May 2011, and two in August 2011. WCH's spawning protocols are described in detail by Barton et al. (2012), and by Waldbusser et al., (2013). Briefly, larvae are maintained in static 22 m^3 tanks, which have their water changed every 2-3 days, and are fed daily (Table 1). The water for each tank change is pumped from Netarts Bay — a marine-dominated estuary on the northern Oregon coast (45.403 °N, 123.944 °W). The bay is flushed nearly every tidal cycle with water from the adjacent North Pacific Ocean and receives very little freshwater input, draining a 36.3 km^2 watershed via several small creeks (Whiting & McIntire 1985). Sub-tidal regions are branching channels and connect near the mouth, and equivalent mean depth and tidal amplitude are both approximately 2 m. With roughly two-thirds of the 9.41 km^2 aerial extent covered in *Zostrera* beds, and the remaining tidal flats supporting production from benthic diatoms, there is a diurnal PCO_2 cycle that reflects the daily cycle of photosynthesis and respiration in Spring and Summer such that the highest PCO_2 values are seen in the morning after a night of respiration and the lowest PCO_2 values are seen in the afternoon, after a day of photosynthesis (Waldbusser and Salisbury, 2014). Thus, the saturation state at the hatchery intake pipe is variable on hourly, weekly and seasonal timescales (Barton et al., 2012, Waldbusser and Salisbury, 2014). For the May cohort, water for each tank-fill was pumped in the afternoon, when PCO_2 was relatively low. To exaggerate the naturally-occurring PCO_2 conditions of the upwelling season in August, water was pumped in the morning. May 2011 was a period of high freshwater input into Netarts Bay

and thus the water started with a lower alkalinity than usual. All water is heated to 25°C before being pumped into the tanks.

Spawn and Larval Culture

On 18 May 2011 and again on 14 August 2011, at least 3 Willapa Bay females were strip-spawned and fertilized with sperm from at least one Willapa Bay male. The fertilized eggs in August were split into two different tanks ~ 1 hr after fertilization (a "buffered" and control, each starting with approximately 400 million larvae), and followed separately for the remainder of their larval period. In 2011, WCH buffered incoming water with industrial grade soda ash (Na_2CO_3) to counter the elevated PCO_2 during summer upwelling. Target buffering levels were set to reach Ω_{arag} greater than 4 (Table 2, Fig 1.).

All larvae were fed a rotating mixture of algal cultures grown at WCH including *Isochrysis sp.*, *Chaetoceros gracilis*, and *Chaetoceros calcitrans* (Table 1). In the first 5-10 days the larvae were fed *Isochrysis sp* from a continuous culture bag system and these algae have a particularly low $\delta^{13}C$ signal [around -45‰], due to the bubbling of culture water with compressed CO_2, which can be seen in Fig. 3. At each feeding, between 200 and 800 mL of algae were filtered onto pre-combusted 47mm GF/F glass fiber filters (Whatman) and dried for storage at <45°C. The sample volume was determined to account for different densities of algal culture and achieve optimal amounts of organic material on each filter for analysis.

My thesis employs a latitudinal study design by sub-sampling the cohort/population at each tank water change. At each change, the previous tank was drained onto an appropriately sized sieve to capture all the larvae, and the larvae then transferred into a newly-filled tank. A 0.5 – 2 g dry weight sub-sample (representing an estimated 3-10 × 10^6 two-day old larvae or 2 - 9 × 10^5 19-day old larvae) of the cohort was collected from the sieve, briefly rinsed with DI water and immediately frozen. The samples were then freeze-dried within three weeks of collection (Labconco FreeZone 6 Freeze Drier). As all the larvae from each cohort were living in the same tank, taking multiple primary samples would have been pseudo-replication, and I assume that the

primary samples accurately represent the entire larval cohort. In May, after 5 days, the fastest growing larvae were selected by passing the cohort through an 80 µm sieve, which caught about half of the larvae. This is a common procedure at WCH with poorly performing cohorts. The August cohorts were not sorted via this size-fraction screening.

Isotopic and Compositional Measurements of Larvae and Algae

All stable carbon isotope (^{13}C, expressed as $\delta^{13}C$) samples were analyzed in Oregon State University's College of Earth, Ocean, and Atmospheric Sciences Stable Isotope Laboratory. Detailed descriptions of these standard protocols can be found in Waldbusser et al., (2013) and at http://stable-isotope.coas.oregonstate.edu/. All runs were calibrated and checked with NIST certified and in-house calibrated standards. Precision and accuracy are noted for each analysis.

To measure larval tissue $\delta^{13}C$ and $\delta^{15}N$, 6-10 mg freeze-dried larvae in Ag boats were acidified in a concentrated HCl atmosphere following the method of Hedges & Stern (1984). The samples were dried overnight, encapsulated in Sn boats, and loaded into a Costech Zero Blank Autosampler. Samples were flash combusted at >1020°C using a Carlo Erba NA1500 Elemental Analyzer (Verardo et al. 1990) and the resulting gas was analyzed by continuous-flow mass spectrometry using a DeltaPlus XL isotope ratio mass spectrometer. Hole punches of filter (diameter ~7mm) with dried algae were analyzed via the same method as the larval tissue, without the acidification step. Repeatability of samples was 0.21‰ for $\delta^{13}C$, and 0.27‰ for $\delta^{15}N$.

In order to measure larval shell carbonate $\delta^{13}C$, I reacted 19-50 freeze-dried larvae with ~105% orthophosphoric acid at 70°C for 5 minutes in a Finnigan Keil III device. The resulting CO_2 was isolated from other reaction products and measured on a MAT 252 mass spectrometer by dual inlet mass spectrometry. Accuracy was better than 0.05‰, and repeatability was 0.02 ‰.

Larval samples were also analyzed for organic and inorganic elemental composition before and after acidification as described above on a Carlo Erba NA-1500 elemental analyzer calibrated with at least 6 acetanilide standards following the methods

of Verardo et al., (1990). Ash-free dry weight (AFDW) was determined by weight before and after combustion at 490°C for 4 hours.

Extractable Lipids, Length and SEM Imaging

At each tank change, an aliquot of larvae were fixed in 2.5% gluteraldehyde and 1% paraformaldehyde in a 0.1 M cacodylate buffer. Samples were later transferred to 50% ethanol and, imaged using an Olympus SZH10 dissecting microscope. 100 larval lengths per sampling point were measured (ImageJ 1.44p). Lengths were converted into weights using the dry-tissue weight to length relationship for larval *C. gigas* from Bochenek et al. (2001), accounting for our measured proportion shell (1-AFDW) at each time point, instead of the 75% shell assumption used by Bochenek et al., (2001).

To measure extractable lipids, ~75 mg samples of freeze-dried larvae were extracted on a Dionex ASE 200 Accelerated Solvent Extractor for four cycles of 5 minutes at 1500 psi with 3:1 methylene chloride: methanol. The extracts were combined with 25 mL hexane and washed against 10 mL 50% saturated NaCl to remove hydrophilic impurities (proteins, carbohydrates). The aqueous phase was drained away and the lipid-containing fraction was dried under an N_2 gas stream. The lipid concentrate was then re-suspended in 500 µL CS_2 and an aliquot (100 µL) moved to a tared stainless steel weigh boat, dried and re-weighed to get a gravimetric weight of lipid. This weight was compared to the original sample weight to find the fraction total lipid. As with the other bulk measurements, these values were normalized to the larval weights to estimate lipid (ng) per larvae. Additionally, it should be noted that the lipid measurements by Waldbusser et al., (2013) may be an over-estimate of true values, due to the gravimetric extraction method used. The washed values presented here are a better estimate of the true lipid content. Due to a sampling error, I do not have a reliable washed lipid value for the 48 hour time point for the May cohort. Given the similarity between the washed and unwashed values in early life, I am using the unwashed gravimetric lipid weight (as reported in Waldbusser, 2013) instead.

Water Samples

       Water samples were collected at each tank filling prior to the addition of larvae or algae. For DIC carbon isotope analysis, aliquots of $HgCl_2$ -fixed sample were pipetted into Labco glass vials sealed with rubber septa caps. The vials were cooled to 13°C, allowed to equilibrate for 15 minutes, and purged with He for 5 minutes each. 85% phosphoric acid was then added to each vial via syringe. The samples were left to equilibrate for 10 hours and analyzed via continuous-flow mass spectrometry using a GasBench-DeltaV system. Each run was standardized using a combination of sodium bicarbonate (3 mM in solution) and calcium carbonate standards. These methods have a precision of 0.15 ‰ and repeatability better than 0.2 ‰.

       Samples for PCO_2 and dissolved inorganic carbon (DIC) analysis were collected at each water change in 330 mL amber glass bottles, poisoned with $HgCl_2$ and analyzed following Bandstra et al. (2006) The uncertainty of these measurements is less than 5% and 0.2% for PCO_2 and DIC, respectively. The remaining carbonate system parameters were calculated using the carbonic acid dissociation constants of Mehrbach (1973) as refit by Lueker et al. (2000), the boric acid constants as defined by Dickson (1990), and the aragonite solubility as defined by Mucci (1983).

SEM Initial Shell Precipitation and Development Study

       On June 4th, 2013, at least three female Willapa Bay female *C. gigas* were strip-spawned and their eggs fertilized with sperm from three Molluscan Broodstock Program males. After checking for fertilization, and rinsing off the excess sperm, the larvae were allowed to develop in Netarts Bay seawater in 4 L glass beakers held at 25°C for 24 hours. Every two hours, ~1000 larvae were collected onto a polycarbonate filter (Whatman 13mm, 5 μm pore size), and fixed in 2.5% gluteraldehyde and 1% paraformaldehyde in a 0.1 M cacodylate buffer. After at least a week, samples were rinsed of fixative with excess buffer. They were then dehydrated in 100% ethanol and transferred into hexamethyldisilazane HMDS. For each dehydration, the samples were transferred though 10%, 30%, 50%, 70%, 90%, and 100% ethanol or HMDS with 20 minutes per rinse. Then the samples were air-dried from the HMDS for 24 hours, sputter-

coated with a gold palladium mixture and imaged with a FEI Quanta 600F Environmental
SEM to examine the development of the initial shell.

Statistical Analyses and Isotope Calculations

      In these cohorts, the stable isotopic composition of shell, larval tissues, and food
were used as tracers of carbon and nitrogen during larval shell formation and
development. Stable nitrogen and carbon isotopic data provide independent estimates of
the rate of incorporation of exogenous food into larval tissue. The estimate is a function
of the feeding rate (gain) and the catabolism of energy stores (loss). Thus, a simple mass-
balance of organic carbon (OC) and nitrogen (ON) was constructed. Isotope values of the
tissue at each time point and the algal diet were used to constrain the model and to
calculate a mass loss (e.g., respiration, excretion) and a mass gain (e.g., assimilation) of
both OC and ON during each tank change until the tissue began to overlap with the algae
signal.

      The carbon and nitrogen isotope ratios of the larval tissue at each tank change
were each mathematically described below, using organic carbon (OC) as an example,
The system of equations was solved for m_{loss} and m_{gain}: the weight of OC (or ON) lost
and gained respectively during each tank incubation (i.e., between t_{-1} and t_0).

$$\delta^{13}C_{t_0} = \left(f_{remain}\delta^{13}C_{t-1}\right) + \left(f_{gain}\left(\delta^{13}C_{algae} + \Delta\right)\right)$$

$$m_{t_0} = m_{t-1} - m_{loss} + m_{gain}$$

$$f_{remain} = \frac{m_{t-1} - m_{loss}}{m_{t_0}}$$

$$f_{gain} = \frac{m_{gain}}{m_{t_0}}$$

When solved,

$$m_{loss} = \frac{m_{t_0}\left(\delta^{13}C_{t_0} - \left(\delta^{13}C_{algae} + \Delta\right)\right) + m_{t-1}\left(\left(\delta^{13}C_{algae} + \Delta\right) - \delta^{13}C_{t-1}\right)}{\left(\delta^{13}C_{algae} + \Delta\right) - \delta^{13}C_{t-1}}$$

$$m_{gain} = m_{t_0} - m_{t-1} + m_{loss}$$

Where $\delta^{13}C_{algae}$ is the mean of the isotope values for all the algal cultures fed during the tank incubation; Δ is the assumed trophic fractionation between diet and tissue; $\delta^{13}C_{t_0}$ is the isotope value of the tissue at the end of the tank incubation; $\delta^{13}C_{t-1}$ is the isotope value of the tissue at the beginning of the tank incubation; m_{t_0} is the mass of OC at the end of the tank incubation; m_{t-1} is the mass of OC at the beginning of the tank incubation; f_{remain} is the fraction of m_{t_0} that was not lost between the beginning of the tank incubation and the end, and f_{gain} is the fraction of m_{t_0} that was gained during the tank change. The initial and final masses for each tank change were calculated by multiplying the measured weight fraction OC or ON by the per larvae weight. Calculations were run in parallel with high and low literature estimates for Δ (McCutchan et al. 2003, Emmery et al. 2011). For N, the low $\Delta^{15}\delta N$ estimate was 2.3‰ while the high estimate was 5‰. The low $\Delta^{13}\delta C$ estimate was 0‰ while the high estimate was 2‰. A mass-specific rate of ON or OC gain or loss was thus calculated for each tank change (not presented). Calcification rate was estimated by normalizing the amount of shell precipitated during each tank change to the total (dry) weight of the larvae at the end of the tank change.

Fraction metabolic carbon in the shell at each time-point was calculated using the method of McConnaughey et al. (1997) using the inputs of tissue $\delta^{13}C$ to approximate the respired carbon in the calcifying fluid, the $\delta^{13}C$ of the ambient DIC during the most recent tank change, and the $\delta^{13}C$ of the larval shell. The abiotic equilibrium fractionation between aragonite and bicarbonate (Δ) was taken from (Romanek et al. 1992).

$$R\left(\delta^{13}C_{resp}\right) + (1 - R)(\delta^{13}C_{DIC}) = \delta^{13}C_{Shell} - \Delta$$

Where R is the proportion of metabolic contribution to shell, $\delta^{13}C_{resp}$ is the isotope value of respired carbon approximated from larval organic tissue; $\delta^{13}C_{DIC}$ is the isotope value

of the ambient DIC; $\delta^{13}C_{Shell}$ is the isotope value of the shell, and Δ is the abiotic fractionation between aragonite and bicarbonate (Romanek et al., 1992).

All statistical analyses were done in the statistical program "R" (2.15.2), and used the package "multcomp".

RESULTS

The experimental conditions for both cohorts were variable, but within the observed range of variability in Netarts Bay, Oregon (Barton et al., 2012). Mean carbonate chemistry conditions in May were characterized by near-atmospheric PCO_2 and a moderate Ω_{arag} of 2.6, while upwelling in August generated a higher mean PCO_2 and mean Ω_{arag} of 1.6. (Fig. 1, Table 2). In general, the August unbuffered cohort saw high PCO_2 water with a correspondingly low saturation state, although upwelling intensity varied over the 21 day period and was strongest between 5 and 10 days post fertilization. The August buffered cohort experienced the same upwelled water, but it was buffered to decrease the PCO_2 and increase Ω_{arag}, and these differences can be seen in their respective PCO_2 and Ω_{arag}. A one-way ANOVA showed significantly different mean Ω_{arag} among cohorts, $F(2, 27) = 219$, p = <0.0001, and a post hoc Tukey comparison of the three groups indicated that all comparisons are significant when $\alpha = 0.05$. The lowest mean tank saturation state was seen in the August unbuffered tanks, while the highest was seen in the buffered tanks, with the May tanks having an intermediate mean saturation state. The initial tank conditions, (seen in Table 2), for all cohorts were over the ~1.6 Ω_{arag} threshold for larval success identified by Barton et al. (2012). On average, the change in saturation state over each tank change was <0.3. The largest change in saturation state over the course of a tank incubation occurred in the August unbuffered cohort during the 5th tank incubation [0.55 change in Ω_{arag}, accompanying a ~660 µatm decrease in PCO_2]. This is not unexpected, as the PCO_2 values started the furthest from atmospheric equilibrium during the most intense upwelling.

Mean shell length (a proxy for growth) was similar among all three cohorts, while soft tissue proxies such as such as ash-free dry weight (AFDW), lipid bulk, and C:N ratio of tissue were more variable (Figure 2). In all cohorts, the lipids were drawn down rapidly during the first 2-5 days, reached a low 5-10 days after fertilization and then were

built up again as the larvae began to accumulate tissue mass from assimilating algae. Maximum per larva lipid stores were seen 19 days after fertilization for all cohorts, which was our last time point for the May cohort and one time point before the end of the study for the August cohorts. I ended the study when most of the cohort reached the settlement size metric used at Whiskey Creek Hatchery.

The lipid fraction of AFDW was similar for the two August cohorts, which came from the same spawn. In contrast, the May cohort, despite having a higher lipid fraction than the two August cohorts, had a lower per larva lipid mass, the result of the May cohort's relatively low AFDW and slightly smaller mean weight. I used CHN elemental analysis of decalcified larvae as an independent check of the lipid proportion (Figure 2), assuming that the three major bulk biochemical components of larval mass are carbohydrate, lipid and protein, and that carbohydrate is a minor constituent (e.g., His & Maurer 1988, Moran & Manahan 2004) Under these assumptions, an elevated C:N ratio indicates a greater lipid:protein ratio. During prodissoconch I (0-2 days), all cohorts had a relatively high mean C:N atomic ratio of around 5.6, and this ratio decreased with age until ~10 days, after which point C:N values in the May cohort started to increase while both August cohorts showed a decrease, presumably suggesting greater accumulation of protein relative to lipids. Note that total organic content was higher in the August cohort (Figure 2).

Calcification rates were similar among all cohorts, and decreased as a function of age as described in Waldbusser et al., 2013. Earlier measurements showed the same pattern (Maeda-Martinez et al., 1987). The highest rates [~0.6 day^{-1}] were seen during the formation of the initial shell (0-1 days), and decreased rapidly to reach a near-constant rate (~0.1 day^{-1}) between 5 and 21 days after fertilization.

In Figure 3, the top panels show $\delta^{13}C$ of the larval shell, larval tissue, algal food source, and DIC during each incubation period (tank change), while the bottom panels show $\delta^{15}N$ of the larval tissue and algae. All cohorts show decreasing shell $\delta^{13}C$ with time, which could indicate either an increasing fraction of metabolic carbon in the shell or that the metabolic carbon being incorporated is becoming lighter (as the tissue from which it is derived approaches the lighter algal food source). These effects can be

disentangled using a two end-member mixing model (McConnaughey 1997). All cohorts show an increasing fraction metabolic carbon with time but there are differences among the cohorts in their estimated incorporation of metabolic carbon (Figure 4). It appears that these differences reflect other measures of condition such as AFDW, and lipid content.

The initiation of feeding is seen as the rapid decrease in $\delta^{13}C$ as the tissue of the larvae starts to reflect the exogenous food source — most noticeable in the August cohorts, where the earliest samples were taken more frequently than in May. Indeed, the August cohorts were sampled at fertilization and when they were one day old and the embryogenesis period can be seen between these time points, as the larvae have not yet begun to feed. In all cohorts, the tissue reflects the algal nitrogen source more slowly than the algal carbon source, indicating that the turnover of carbon is faster than the turnover of nitrogen. Given the greater C:N of lipids relative to protein (and that carbohydrates are usually a very small fraction of the OM), this implies that the larvae are preferentially using lipid as an energy source in early life. In general, the calculated turn-over (both loss and gain) of ON was roughly three times less than the calculated turn overs of OC.

The initial shell formation period is documented via SEM microscopy in Figure 5. At 10 hours, the pellicle (precursor to the prodissoconch I periostracum) loosely covers each incipient valve (Kniprath, 1980, Carriker, 1996). Between 14 and 16 hours, the initial shell is precipitated rapidly from the calcifying space between the pellicle and the shell field epithelium, which later develops into the shell-forming mantle. By 16 hours, the initial shell is completely formed, and the D-hinge shape of the prodissoconch I is clearly visible.

DISCUSSION

The goal of this work was to measure the biological response of the larvae of cultured oyster species, *C. gigas*, to a representative subset of the variability in the carbonate system seen on the Oregon Coast. The study was conducted on multiple commercial cohorts at WCH, where carbonate chemistry is set by the ambient Netarts Bay conditions, but food availability and temperature are controlled. The large (~400 million larvae) cohorts provided sufficient larvae to measure bulk biochemistry parameters such as organic matter content and composition while the sequential tank

incubations allowed us to fully constrain the possible isotopic sources for incorporation into shell and tissue at different intervals during larval life (e.g., 0-2 days, 2-5 days). The ontogenic changes in carbon stable isotope composition observed here have not been well documented before in bivalve larvae, other than by Waldbusser et al. (2013) who presented data from the May cohort. Further, to our knowledge, these are the first investigations of nitrogen stable isotope incorporation in early larval *C. gigas* tissue. The data for the August cohorts further support the patterns described previously (Waldbusser et al. 2013) and contribute new information on the initiation and rate of feeding, the relative turnover of carbon and nitrogen-rich tissues throughout the larval period, and the persistence of patterns in the incorporation of metabolic carbon into early shell.

All cohorts dramatically reduced their AFDW and lipid content in early life, as they catabolized maternally-derived lipids and precipitated inorganic shell. The August larvae were ~60% shell by weight after 24 hours, and ~80% shell by weight after three days. The May cohort had a lower total AFDW, and reached ~88% shell by weight in only two days. The lower lipid content and lower tissue weight in the May cohort compared to the unbuffered August cohort is the opposite of what I anticipated given the typically low saturation state of Netarts Bay in August due to upwelling (e.g., Barton et al., 2012). The unbuffered (control) August cohort was living under moderate acidification stress caused by upwelling, which might be expected to increase lipid utilization as shown by Talmage & Gobler (2011). However, the similarity between the growth of the non-buffered and buffered August cohorts demonstrates that given spawning conditions with a sufficiently high saturation state (Ω_{arag} during prodissoconch I shell formation for the August unbufffered cohort was 2.1), additional improvements in carbonate chemistry conditions in the late larval period do not necessarily improve outcomes, as measured by growth, feeding rate, and biochemical measures of energetic reserves. Here I discuss other factors that could have contributed to the success or failure of each cohort.

I am confident that these measurements accurately reflect the population mean at that time of each sampling, in part because of coherence of our independently measured responses at the different time points. For example, at the 17 day time-point in the May

cohort, the carbon and nitrogen in the tissue become more enriched in light isotopes, reflecting the lighter value of the algae during the most recent tank incubation.

Key factors influencing larval success are well known, among them food availability, environmental conditions, and egg lipid content or other "maternal effects" (Gallager & Mann 1986, Kennedy 1996, Bochenek et al. 2001). *C. gigas* eggs range in diameter from 30 μm to 80 μm, with a typical diameter of 55 μm (Breese & Malouf 1975). In general, egg quality is associated with egg size, however these two are not always correlated (see discussion in Moran & McAlister 2009 and references therein). It is well known that there is variability among egg quality seasonally, or in response to conditioning (Muranaka & Lannan 1984, Gallager & Mann 1986). Although I was not able to measure the weight of the eggs for either cohort, based on the remaining organic material at day 1, and an estimated average OC consumption of ~ 4 ng day^{-1} for the 1 and 2 day old larvae, which was calculated from relevant respiration rates in Gerdes (1983), I estimated that eggs were ~52 ng egg^{-1} in May and ~82 ng egg^{-1} in August. The August cohort eggs had a lipid fraction of AFDW of ~26%, meaning that the per-egg lipid reserves were near the top end of the range of reported literature values (Gallager et al. 1986, Massapina et al. 1999, Uriarte et al. 2004). May egg lipid fraction was not measured, but the egg mass and therefore total lipid content is estimated to be near the low end of reported values, even if I assume a similarly high lipid proportion to the August cohorts.

The calculated per-larvae lipid mass for the May cohort 5 days after fertilization [~2 ng larva^{-1}] is no more than expected from their structural lipids (Moran and Manahan, 2004), which suggests that the larvae had used up all their energy stores. One reason for this could be a low starting egg lipid content as calculated above, which can limit larval growth and survival (Gallager and Mann, 1986; Bochenek et al., 2001). Another potential factor influencing the cohorts was salinity – *C. gigas* larvae are hardy over a range of salinity conditions (e.g., His et al. 1989, Bochenek et al. 2001) spanning those seen in May (23.8 – 30.1). However, the May cohort experienced an instantaneous change in salinity between tank changes at 8 days (from 29.7 to 24.9). This rapid salinity change likely altered their energetic budget; Richmond & Woodin (1996) found that *Ilyanassa*

obsolete larvae exposed to episodic low salinities both grew slower and swam less.Marine invertebrates are more tolerant of salinity changes when they happen gradually (Barnes 1953). Even storm-induced changes in estuarine salinity usually happen over hours, not minutes.

Despite their low lipid content and AFDW, the May cohort did not have significantly growth from the two August cohorts (Figure 2). One reason for this could be WCH's screening procedure, which was done to deal with "poor" performance, and is described in methods. At 11 days, the May cohort was screened on an 80 μm screen, roughly splitting the cohort in half, and I continued to follow only the +80 μm half. In contrast, the August cohorts were never screened, so the measurements presented here reflect the whole population, not just the more successful larvae. Additionally, I do not have data on how many larvae from each of these cohorts successfully made it through metamorphosis, or how they fared throughout juvenile life and into adulthood, but evidence from longitudinal studies suggests that there might have been differences in growth or survival past settlement (Pechenik, 2006, Hettinger et al., 2013, Parker et al., 2012).

Many invertebrates have stage-based instead of time-based milestones for larval development – that is, the length of the larval period is plastic. Stressed larvae tend to spend more time in the planktonic state (reviewed by Gazeau et al 2013, with regards to OA), which means that slower growth can be confused with the achievement of developmental milestones when measuring things like size and shell weight at intervals after fertilization. Even if there are no easily measureable effects of a stressor on live larvae, slowed development can increase larval mortality simply by increasing the amount of time that larvae spend in vulnerable stages.

At 5 days, there is a "low" in organic matter, and lipid stores; a similar pattern in lipid concentrations was seen by His & Maurer (1988) in a wild population of *C. gigas*. There was also a slight decrease in lipid accumulation, growth rates and AFDW between 10 and 15 days for all cohorts (Fig. 2). This period is after the end of the calculated the maternal energy stores (Waldbusser et al., 2013) and perhaps analogous to a trend of decreased survivorship between 14-19 days that was noticed by (Matias et al. 2011) in

the clam *Ruditapes decussatus*, which the authors attributed to decreased feeding and increased biochemical demands associated with preparing for settlement. Although conflicting data exist, it has been recognized that protein stores are important for larvae to successfully metamorphose (e.g., García-Esquivel et al. 2001). The decreasing C:N ratio of the two August cohorts in later larval life, which indicates that these cohorts were increasing their proportion protein compared to lipid or carbohydrates, could be a result of the larvae accumulating proteins prior to metamorphosis. The coincident drawdown of lipid stores could indicate that lipid energy reserves were being catabolized to prepare for metamorphosis. In contrast, the high lipid content in larvae at 19 days in the May cohort could be representative of slowed development due to stress; they may not yet have begun to prepare biochemically for metamorphosis when I stopped following them. Or it could be because the larvae were screened to follow only the largest of the larvae as discussed above. A final explanation for the high late-larval lipid content could be compensatory growth (Metcalfe & Monaghan 2001, discussed in Hettinger et al., 2013). The May cohort larvae could have accelerated their feeding and lipid accumulation to "catch-up" with normal development rates.

There is a persistence of isotope patterns across cohorts, suggesting that I am documenting a relatively conserved pattern in early larval shell development. Shell $\delta^{13}C$ from the May cohort showed increasing incorporation of metabolic carbon into larval shell with age (Waldbusser et al., 2013), indicating greater reliance on ambient DIC during the formation of the initial, or D-hinge shell and suggesting a mechanism of greater vulnerability to the speciation of ambient DIC during this period. The data from the two August cohorts show a similar pattern of increasing metabolic carbon incorporation in shell with age; all observed cohorts appear to be relying less on ambient DIC to build their shell during later larval life than early larval life. Where the cohorts differ is in their incorporation of metabolic carbon during the initial shell formation period (0-5 days). In the raw isotope data, this difference can be seen as the slope of the initial decrease in shell carbon signal (Figure 3), and in the calculated fraction metabolic carbon in shell of Figure 4. The two cohorts with the highest mean tank saturation states – the May cohort, and the August buffered cohorts – both show a continuously increasing

fraction metabolic carbon with time, while the August unbuffered cohort starts with a higher fraction metabolic carbon, and decreases to a minimum incorporation of metabolic carbon at 7 days, and had a steadily increasing metabolic contribution from 7 days until I stopped following the cohort at 21 days. Lorrain et al. (2004) suggested that the ratio of respired to precipitated carbon is responsible for driving patterns of metabolic isotope incorporation in shell for *Pecten maximus*, and the patterns that we've observed are consistent with this. In general, the August cohorts were characterized by higher AFDW and therefore should have higher metabolic carbon production (Gerdes 1983; Hoegh-Guldberg & Manahan 1995). In general, these estimated contributions of metabolic carbon are consistent with those found by Owen et al. (2008) for larval *Placopecten magellanicus*. The observed changes in shell $\delta^{13}C$ integrate all previous time points so the changes in metabolic contribution that I have modeled are less than what I assume the change must be in the newly precipitated shell during these periods.

The highest rates of shell calcification were found during the formation of the initial shell for the August cohort (Fig. 2), confirming the experimental results of Maeda-Martinez et al., (1987), who measured the fastest rates of shell precipitation during the formation of the D-hinge shell for *C. gigas*. The initial shell formation occurs rapidly between 13 and 16 hours, and is structurally and compositionally distinct from later shell Waller 1981, Yokoo et al. 2011). Waldbusser et al., (2013) suggest acidification-caused energetic stress in early larval life as a mechanism of legacy effects, arguing that the energetic stress is likely caused by higher energy expenditure on initial shell formation via the increased production of shell matrix proteins or ion pumping to overcome the kinetic constraint (*sensu* Waldbusser et al., 2013). The relative role of these two processes in maintaining calcification rates under reduced saturation state is still unknown, but the finding of high ambient DIC carbon incorporation in early shell (low metabolic carbon incorporation) suggests greater connectivity between ambient seawater carbonate chemistry and the calcifying fluid during this period, strongly suggesting that ion pumping is not well developed at this stage. Another possible mechanism of sensitivity that would impact the scope for growth is delayed or impaired feeding, which

would reduce availability of exogenous "new" energy (e.g., Vargas et al. 2013; Melzner et al., 2011).

Starvation experiments with bivalve larvae have shown that without exogenous food inputs, survival is possible far beyond the calculated exhaustion of maternally-derived energy and dissolved organic matter (DOM) is the most frequently suggested alternate food source for larvae under such starvation conditions (Moran & Manahan 2004, Tang et al. 2006, Matias et al. 2011). In my thesis so far, I have made the assumption that the larvae act as a "closed" metabolic system (e.g., Bochenek et al., 2001, Emmery et al. 2011). In order to assess how much OC the larvae could obtain, from DOC, I calculated how much dissolved organic carbon (DOC) the larvae would have had access to compared to their requires for respiration and growth. Maximum DOC concentrations in coastal waters are ~105 µM (Hill & Wheeler, 2002), or 12.6 µg DOC mL^{-1}. At WCH, typical stocking densities are 20 larvae mL^{-1} as fertilized eggs, and 5 larvae mL^{-1} as veligers, so DOC available was calculated by the amount of DOC per volume of SW available to each larvae at each tan stocking density. Minimum OC demand was calculated by assuming a baseline (starvation) respiration rate from Moran & Manahan (2004), and adding the calculated increase in OC per larva during each tank incubation. The fraction of the demand that the DOC could fill depended on the density of larvae, the life-history stage and the number of days in each tank. The DOM could have provided ~20 times the total carbon demand in the first 5 days after fertilization, but in later larval life, (just before metamorphosis) the maximum that it could have provided is 80% of the total carbon demand. I therefore conclude that if they were able to access it, there is enough DOC in the system to sustain the larvae, especially in early larval life. However, uncertainties remain about how much of the DOC in seawater would actually be available to the larvae. For example, this calculation assumes that all of the DOM in the incoming seawater is available to the larvae, but an estimated ~40 µM of marine DOC is refractory (Druffel et al. 1992).

If the larvae are using DOC to fuel their growth and respiration, and if the DOC is sufficiently different from the larval samples in isotopic ratio, it could bias the isotope modeling results presented earlier. Estimates of the $\delta^{13}C$ and $\delta^{15}N$ of DOM in the open

Pacific and/or California Current System range from -21‰ to -23‰ for $\delta^{13}C$ and 6.7-9.7‰ for $\delta^{15}N$ (Benner et al. 1997, Bauer et al. 1998, Walker & McCarthy 2012) – closer to our "maternal" egg signal than to the food source. Therefore, I assume that any bias created by the incorporation of DOM would overestimate the contribution of maternal lipid to the total larval energy budget.

CONCLUSIONS

In this study, I followed three cohorts of *C. gigas* larvae from fertilization through settlement at Whiskey Creek Shellfish Hatchery, in Netarts, Oregon. Many patterns in growth and development were conserved among the cohorts, but they differed in several key respects which I primarily attribute to differences in maternal investment. All larvae were raised in water with a high (Ω_{arag} >2) saturation state during the formation of the Prodissoconch I shell, and were therefore not exposed to the sub-lethal ($1>\Omega_{arag}>1.6$) levels of OA stress described by Barton et al., (2012). Developmental patterns in lipid catabolism, bulk composition, and calcification rate among the three diverse cohorts re-enforce the idea that the creation of the initial shell is energetically expensive and that the major energetic source during this period is maternally-derived egg lipids. SEM images documenting the rapid initial shell formation between 10 and 16 hours visually demonstrate the rapid early shell accretion in early larval life. All cohorts reflected the carbon signal of their food source more rapidly than the nitrogen of the food source, indicating that they were catabolizing lipid rapidly in early life. This is corroborated by the corresponding decrease in AFDW, lipid ratio, and the decreasing C:N ratio of their tissue during this period. Shell carbon isotopes of all cohorts showed a decreasing dependence on ambient DIC carbon with time, although differences in the incorporation of metabolic carbon in the initial shell are seen between the buffered and unbuffered August cohorts.

The major factor influencing the observed differences among the cohorts is suggested to be maternal investment (e.g., egg lipids) and not exposure to low saturation state water (OA). I infer that the May cohort likely did have a lower maternal investment, because they had very little lipid reserves by 2 days post-fertilization. They also experienced a salinity shock at 8 days which could have impacted them energetically.

The lower energetic budget of the May cohort can be seen in their lower AFDW, fraction lipid, and feeding behavior. In general, the May cohort did not isotopically reflect their food source as rapidly as the August cohorts, indicating slower feeding, higher metabolic demand or lower maternal energy investments.

Waldbusser et al., (2013) suggest that the primary mechanism of failure in WCH larvae exposed to high-CO_2 water is related to the greater energetic cost of precipitating the initial shell under low saturation states compared to high saturation state conditions. Greater exposure to ambient water carbonate chemistry during this critical period means that under acidified conditions, larvae must expend extra energy to overcome the kinetic demand. This energetic insult occurs before larvae start incorporating exogenous food, and reduces their subsequent scope for growth, which is a key link between exposure in early life and the observed failures in the later larval period.

Table 1. Algal culture composition for May and August cohorts. Both cohorts in August received the exact same algal cultures in the same ratios, and are therefore presented in this table combined.

Age	May	August	Key to algae types
0	-	-	CISO: *Isochrysis sp.* (Caribbean)
1	-	CISO	bbsCISO: CISO in bag system
2	CSIO + CCP + bbsCISO	bbsCISO	TISO: *Isochrysis sp.* (Tahitian)
3	bbsCISO	bbsCISO	NANO - *Nannochloropsis sp.*
4	bbsCISO	bbsCISO	CG - *Chaetoceros gracilis*
5	bbsCISO	bbsCISO	CCP - *Chaetoceros calcitrans*
6	bbsCISO	CISO	3H - *Thalassiosira pseudonana*
7	bbsCISO	CISO	blend - in-house mix of taxa
8	bbsCISO	CISO + TISO	
9	blend + CISO	CISO	
10	CISO	CISO + TISO	
11	blend + CISO	CISO + TISO	
12	CSIO + CCP	bbsCISO	
13	blend	CISO + CCP	
14	blend + NANO + CCP	-	
15	CISO + NANO + CCP	CG + CCP + CISO	
16	CISO	CG + CISO	
17	CISO + CCP	CG + CISO	
18	TISO	CG + CISO	
19		CG + CCP + CISO	
20		CISO	
21		CG + 3H	

Table 2. Mean carbonate chemistry of tank incubations for each cohort ± SD. Tanks were heated to ~25°C prior to each tank filling, and rarely cooled to less than 23°C between tank fillings.

	Salinity (psu)	PCO_2 (µatm)	Talk (µeq kg^{-1})	DIC (µM kg^{-1})	Mean pH$_{sws}$	Mean Ω_{arag}	Ω_{arag} at spawn
May (n=8)	26.6 ± 2.3	364 ± 40	1991 ± 78	1758 ± 50	8.04 ± 0.04	2.6 ± 0.3	2.4
August (11)	32.7 ± 0.6	1008 ± 207	2318 ± 151	2181 ± 68	7.71 ± 0.16	1.6 ± 0.2	2.1
August trt (11)	32.8 ± 0.6	425 ± 45	2842 ± 91	2452 ± 81	8.09 ± 0.04	4.2 ± 0.3	4.6

Table 3. Stable isotopes of carbon (δ¹³C VPDB) and nitrogen (δ¹⁵N) from tissue, shell and diet of all three cohorts. All analyses were completed in CEOAS Stable Isotope Laboratory following standard analytical protocols. Both cohorts in August received the exact same algal cultures in the same ratios, and are therefore presented in this table combined.

Days Since Fertilization	Tissue δ¹³C			Tissue δ¹⁵N			Algae δ¹³C		Algae δ¹⁵N		Shell δ¹³C			DIC δ¹³C		
	May	Aug.	Aug. (trt)	May	Aug.	Aug. (trt)	May	Aug.	May	Aug.	May	Aug.	Aug. (trt)	May	Aug.	Aug. (trt)
0		-20.00	-20.00		9.87	9.87									-0.12	-0.52
1		-19.48	-19.38		10.10	10.12		-35.77		-6.48		0.75	0.65		-0.03	-0.46
2	-19.55			9.58			-39.47	-50.19	-8.66	-2.81	1.33			-0.04		
3		-29.46	-29.73		5.07	4.98	-46.58	-47.15	-7.60	-2.96		-0.04	-0.44		0.03	-0.52
4							-46.42	-47.01	-7.52	-2.79						
5	-23.60	-32.84	-33.57	5.05	3.97	3.62	-46.49	-47.13	-7.21	-3.59	0.96	-0.13	-0.72	-0.04	-0.17	-0.77
6							-45.38	-30.16	-5.67	-5.60						
7		-34.17	-34.44		2.94	2.11	-45.79	-32.97	-5.82	-6.15		-0.25	-1.03		-0.29	-0.81
8	-30.80			2.00			-45.42	-39.91	-4.96	-5.75	-0.18			-0.61		
9		-32.92	-32.96		1.05	0.47	-27.85	-37.57	-10.44	-5.74		-0.43	-1.26		-0.31	-1.06
10							-33.89	-35.82	-12.71	-6.04						
11	-30.32	-33.15	-32.95	-0.73	-0.47	-0.96	-29.04	-32.48	-9.74	-6.24	-0.95	-0.79	-1.61	-0.15	-0.49	-0.92
12							-26.89	-50.96	-5.11	-3.09						
13	-28.14	-34.23	-33.94	-3.34	-0.99	-1.38	-26.76	-40.37	-5.60	-6.50	-1.03	-1.34	-2.14	0.10	-0.08	-0.56
14							-34.38	-53.80	-9.35	-4.59						
15	-28.10	-34.76	-34.66	-3.09	-1.79	-2.08	-38.49	-37.70	-11.41	-7.59	-1.00	-1.50	-2.35	0.37	-0.27	-0.97
16							-43.19	-33.32	-7.81	-4.69						
17	-32.95	-33.90	-33.74	-5.18	-1.83	-2.19	-31.95	-33.32	-4.75	-5.17	-1.40	-1.62	-2.60	0.18	-0.09	-0.58
18				-4.92			-35.38	-34.73	-12.15	-4.52						
19	-27.31	-33.18	-33.14	-2.64	-2.37	-2.61		-44.41		-4.32	-1.05	-1.69	-2.74		-0.02	-0.51
20								-36.64		-5.64						
21		-33.97	-34.04		-2.81	-2.94						-1.90	-2.91			

Table 4. Biochemical properties of larvae, organic matter, and diet of all three cohorts.

Cohort	Days Since Fertilization	Fract. Lipid (wt/wt)	Fract. Organic (AFDW)	Mean Length (μm)	stdev Length (μm)	Est. Weight (ng larva^{-1})	Est. Lipid (ng larva^{-1})	Total %N (wt/wt)	Total %C (wt/wt)	Organic %N (wt/wt)	Organic %C (wt/wt)	Tissue C:N (atomic)	Calcif. Rate (day^{-1})
Aug.	0 (eggs)	0.231	0.89	-	-	-	-	-	-	-	-	-	
Aug.	1	0.113	0.4	76	6	172	10	0.05	0.27	0.04	0.18	5.7	0.6
Aug.	3	0.043	0.2	83	6	221	10	0.02	0.19	0.02	0.08	5.2	0.17
Aug.	5	0.011	0.17	90	5	266	3	0.02	0.17	0.02	0.07	5.1	0.09
Aug.	7	0.011	0.16	92	6	282	3	0.02	0.17	0.02	0.07	4.8	0.02
Aug.	9	0.013	0.17	99	13	341	4	0.02	0.18	0.02	0.08	4.9	0.07
Aug.	11	0.019	0.2	122	21	581	11	0.02	0.19	0.02	0.08	5	0.15
Aug.	13	0.023	0.23	125	23	625	14	0.03	0.2	0.03	0.11	4.8	0.01
Aug.	15	0.015	0.23	151	36	1001	15	0.03	0.2	0.03	0.1	4.5	0.15
Aug.	17	0.016	0.25	167	32	1306	21	0.03	0.21	0.03	0.11	4.6	0.08
Aug.	19	0.023	0.27	182	40	1624	37	0.03	0.21	0.03	0.12	4.7	0.07
Aug.	21	0.02	0.26	196	38	1959	38	0.03	0.21	0.03	0.12	4.4	0.06
Aug (trt)	0 (eggs)	0.246	0.92	-	-	-	-	0.09	0.49	-	-	-	
Aug (trt)	1	0.098	0.38	74	5	162	9	0.04	0.27	0.04	0.17	5.5	0.62
Aug (trt)	3	0.035	0.18	85	7	231	8	0.02	0.18	0.02	0.08	4.7	0.19
Aug (trt)	5	0.01	0.16	91	7	279	3	0.02	0.17	0.02	0.07	4.8	0.08
Aug (trt)	7	0.012	0.16	94	9	299	4	0.02	0.2	0.02	0.07	4.5	0.03
Aug (trt)	9	0.008	0.17	107	12	418	5	0.02	0.18	0.02	0.07	4.5	0.11
Aug (trt)	11	0.015	0.19	118	20	530	8	0.02	0.18	0.02	0.08	4.7	0.08
Aug (trt)	13	0.017	0.23	132	26	715	12	0.03	0.2	0.02	0.1	4.8	0.08
Aug (trt)	15	0.014	0.23	156	35	1093	16	0.03	0.2	0.03	0.1	4.6	0.13
Aug (trt)	17	0.014	0.25	173	38	1430	21	0.03	0.2	0.03	0.11	4.6	0.08
Aug (trt)	19	0.017	0.25	201	43	2102	36	0.03	0.21	0.03	0.11	4.5	0.12
Aug (trt)	21	0.014	0.26	214	45	2445	35	0.03	0.21	0.03	0.12	4.4	0.05
May	2	0.023	0.12	77	5	179	4	0.01	0.16	0.01	0.05	5.8	0.44
May	5	0.01	0.08	81	4	205	2	0.01	0.14	0.01	0.03	4.8	0.05
May	8	0.01	0.1	89	7	264	3	0.01	0.15	0.01	0.04	4.5	0.06
May	11	0.017	0.14	106	10	411	7	0.02	0.17	0.02	0.06	4.4	0.09
May	13	0.02	0.18	126	15	631	13	0.02	0.18	0.02	0.08	4.9	0.13
May	15	0.019	0.16	135	17	756	14	0.02	0.18	0.02	0.07	4.9	0.08
May	17	0.033	0.25	144	23	990	33	0.03	0.21	0.02	0.1	4.9	0.05
May	19	0.047	0.32	203	40	2142	101	0.04	0.24	0.03	0.15	5.7	0.17
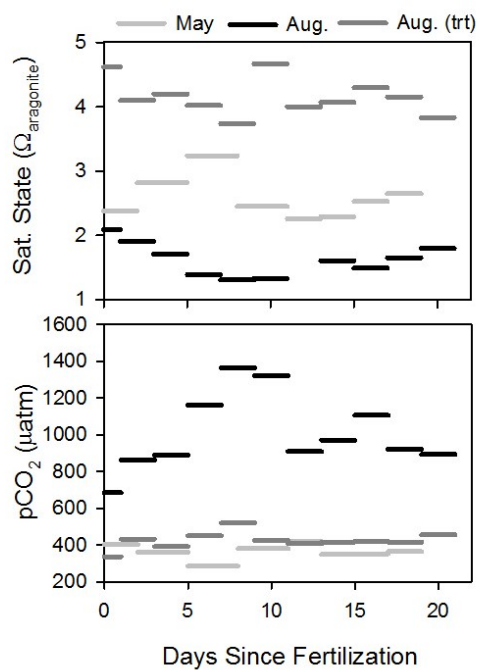
Figure 1. Carbonate chemistry conditions for each tank incubation at Whiskey Creek Sellfish Hatchery, in Netarts Bay, Oregon. Water samples were taken at the beginning of each tank change, just prior to the addition of larvae or algae, and analyzed by standard methods at Oregon State University.
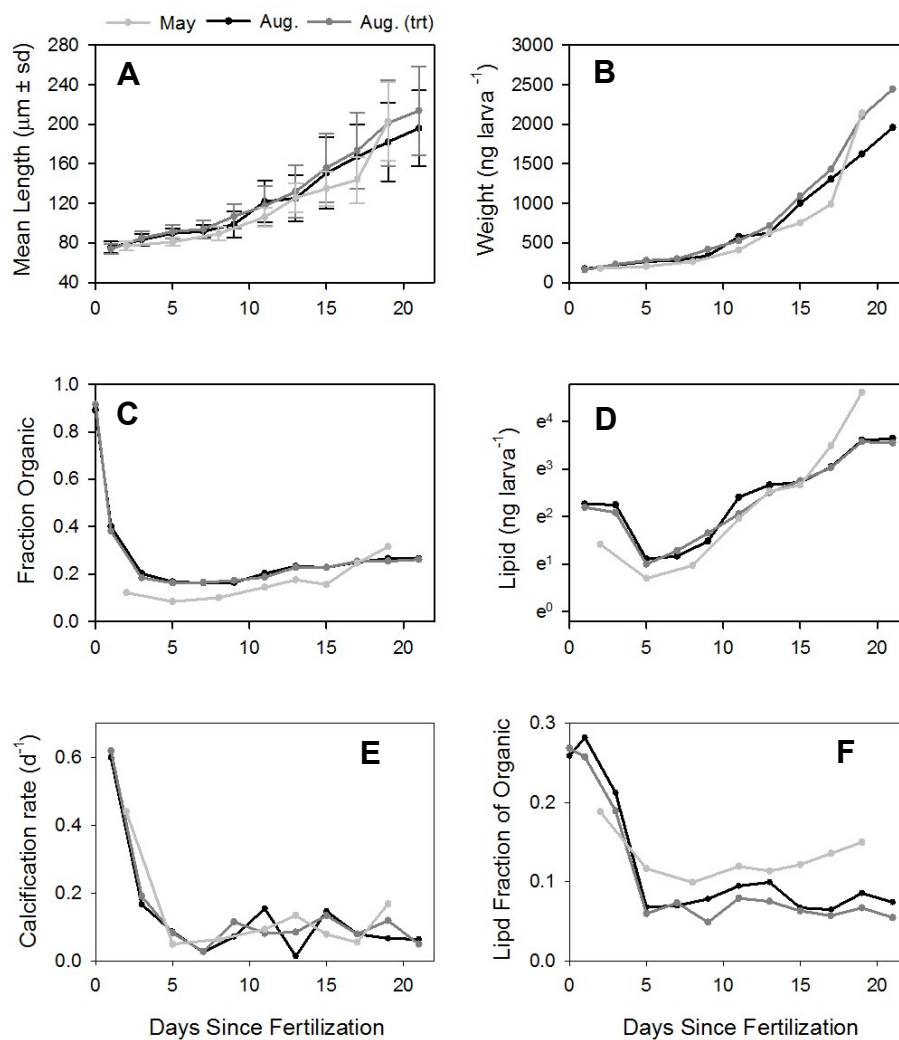
Figure 2. Biochemical measurements of larvae at each tank change. A: Mean length of larvae ± sd. B: Dry weight per larva, calculated using length to dry weight relationship from Bochenek et al., (2001). C: Fraction organic material (AFDW) D: Calculated lipid mass per larvae. (B) and fraction lipid. E: Mass-normalized calcification rate. F: Lipid fraction of AFDW (organic material).
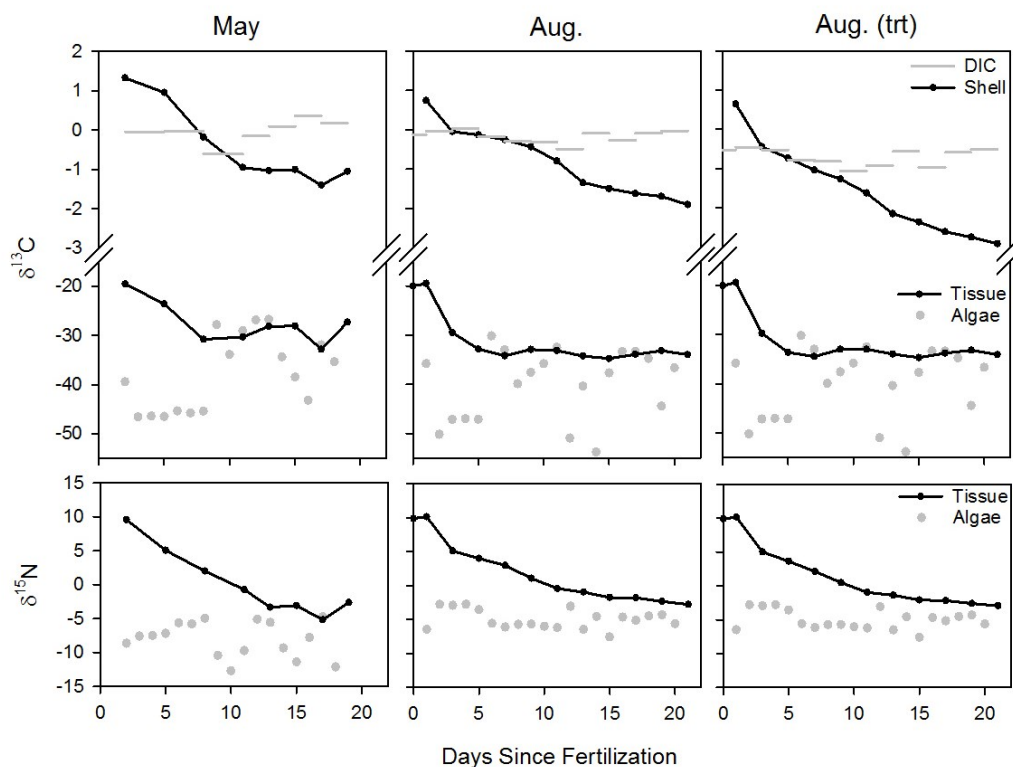
Figure 3. Stable isotopes (δ^{13}C, δ^{15}N) of tissue, shell, ambient DIC and algae. Top panels show stable isotopes of carbon (δ^{13}C) in tank DIC (gray bars), larval shell (black line above break), algae (gray circles), and larval tissue (black line below break). Bottom panels show stable isotopes of nitrogen (δ^{15}N) in algae (gray circles), and larval tissue (black line).
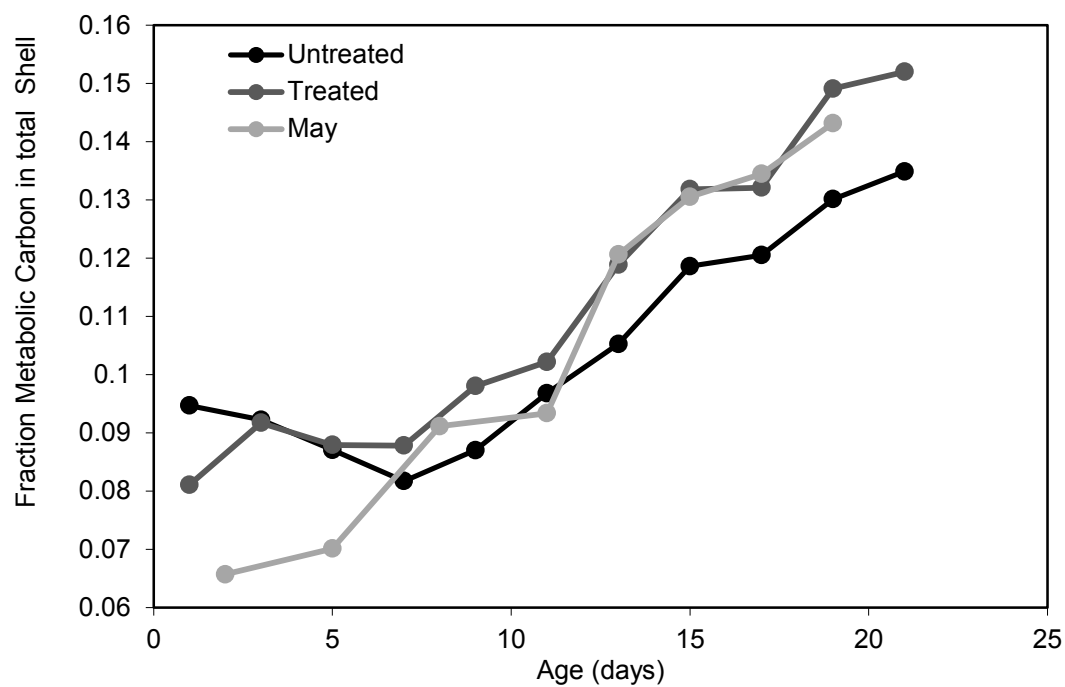
Figure 4. Calculated fraction metabolic carbon in shell for all three cohorts.
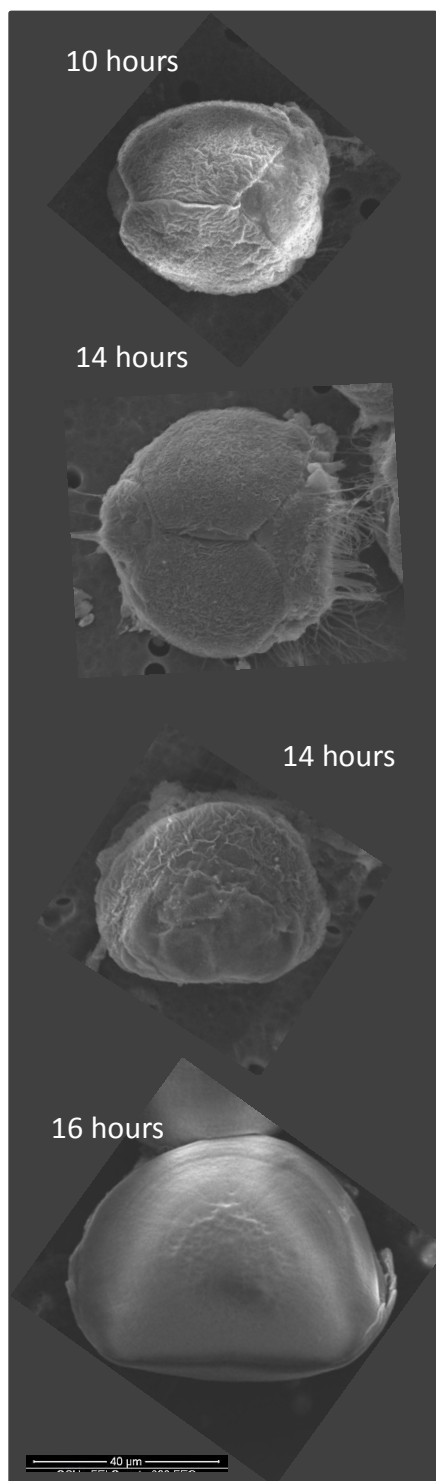
Figure 5 SEM time-series of rapid initial mineralization of D-hinge in C. gigas larvae from Whiskey Creek Shellfish Hatchery. Larvae are from a different cohort than those followed in this manuscript.

BIBLIOGRAPHY

Adelsman H, Whitely-Binder L eds (2012) Washington State Blue Ribbon Panel on Ocean Acidification: Ocean Acidification: From Knowledge to Action, Washington State's Strategic Response. Publication no. 12-01-015. Washington Department of Ecology, Olympia, Washington

Bandstra L, Hales B, Takahashi T (2006) High-frequency measurements of total CO2: Method development and first oceanographic observations. Mar Chem 100:24–38

Barnes H (1953) The Effect of Lowered Salinity on Some Barnacle Nauplii. J Anim Ecol 22:328–330

Barry JP, Tyrrell T, Hansson L, Plattner G, Gattuso J (2010) Atmospheric CO2 targets for ocean acidification perturbation experiments. In: Guide to best practices for ocean acidification research and data reporting. Publications Office of the European Union., Luxembourg

Barton A, Hales B, Waldbusser GG, Langdon C, Feely RA (2012) The Pacific oyster, Crassostrea gigas, shows negative correlation to naturally elevated carbon dioxide levels: Implications for near-term ocean acidification effects. Limnol Ocean 57:698–710

Bauer JE, Druffel ER., Wolgast DM, Griffin S, Masiello CA (1998) Distributions of dissolved organic and inorganic carbon and radiocarbon in the eastern North Pacific continental margin. Deep Sea Res Part II Top Stud Ocean 45:689–713

Benner R, Biddanda B, Black B, McCarthy M (1997) Abundance, size distribution, and stable carbon and nitrogen isotopic compositions of marine organic matter isolated by tangential-flow ultrafiltration. Mar Chem 57:243–263

Bochenek EA, Klinck JM, Powell EN, Hofmann EE (2001) A biochemically based model of the growth and development of Crassostrea gigas larvae. J Shellfish Res 20:243–266

Borges AV (2005) Do we have enough pieces of the jigsaw to integrate CO2 fluxes in the coastal ocean? Estuaries 28:3–27

Borges AV, Schiettecatte L-S, Abril G, Delille B, Gazeau E (2006) Carbon dioxide in European coastal waters. Estuar Coast Shelf Sci 70:375–387

Breese WP, Malouf RE (1975) Hatchery manual for the Pacific oyster.

Carriker MR (1996) The Shell and Ligament. In: Kennedy VS, Newell RIE, Eble AF (eds) The Eastern Oyster : Crassostrea virginica. Maryland Sea Grant College, College Park, Maryland, p 75–168

Dai M, Lu Z, Zhai W, Chen B, Cao Z, Zhou K, Cai W-J, Chen C-TA (2009) Diurnal variations of surface seawater pCO(2) in contrasting coastal environments.

DeNiro MJ, Epstein S (1978) Influence of diet on the distribution of carbon isotopes in animals. Geochim Cosmochim Acta 42:495–506

Dickson AG (1990) Thermodynamics of the dissociation of boric acid in synthetic seawater from 273.15 to 318.15 K. Deep Sea Res Part Ocean Res Pap 37:755–766

Druffel ERM, Williams PM, Bauer JE, Ertel JR (1992) Cycling of dissolved and particulate organic matter in the open ocean. J Geophys Res Oceans 97:15639–15659

Emmery A, Lefebvre S, Alunno-Bruscia M, Kooijman S a. LM (2011) Understanding the dynamics of delta C-13 and delta N-15 in soft tissues of the bivalve Crassostrea gigas facing environmental fluctuations in the context of Dynamic Energy Budgets (DEB). J Sea Res 66:361–371

Evans W, Hales B, Strutton PG (2013) pCO2 distributions and air-water CO2 fluxes in the Columbia River estuary. Estuar Coast Shelf Sci 117:260–272

Feely RA, Sabine CL, Hernandez-Ayon JM, Ianson D, Hales B (2008) Evidence for upwelling of corrosive" acidified" water onto the continental shelf. Science 320:1490

Gallager SM, Mann R (1986) Growth and survival of larvae of Mercenaria mercenaria (L.) and Crassostrea virginica (Gmelin) relative to broodstock conditioning and lipid content of eggs. Aquaculture 56:105–121

Gallager SM, Mann R, Sasaki GC (1986) Lipid as an index of growth and viability in three species of bivalve larvae. Aquaculture 56:81–103

García-Esquivel Z, Bricelj VM, González-Gómez MA (2001) Physiological basis for energy demands and early postlarval mortality in the Pacific oyster, Crassostrea gigas. J Exp Mar Biol Ecol 263:77–103

Gazeau F, Parker LM, Comeau S, Gattuso J-P, O'Connor WA, Martin S, Poertner H-O, Ross PM (2013) Impacts of ocean acidification on marine shelled molluscs. Mar Biol 160:2207–2245

Gerdes D (1983) The Pacific oyster Crassostrea gigas: Part II. Oxygen consumption of larvae and adults. Aquaculture 31:221–231

Gobler CJ, Talmage SC (2013) Short- and long-term consequences of larval stage exposure to constantly and ephemerally elevated carbon dioxide for marine bivalve populations. Biogeosciences 10:2241–2253

Gruber N (2011) Warming up, turning sour, losing breath: ocean biogeochemistry under global change. Philos Trans R Soc Math Phys Eng Sci 369:1980–1996

Harris KE, DeGrandpre MD, Hales B (2013) Aragonite saturation state dynamics in a coastal upwelling zone. Geophys Res Lett 40:2720–2725

Hauri C, Gruber N, McDonnell AMP, Vogt M (2013) The intensity, duration, and severity of low aragonite saturation state events on the California continental shelf. Geophys Res Lett 40:3424–3428

Hauri C, Gruber N, Vogt M, Doney SC, Feely RA, Lachkar Z, Leinweber A, McDonnell AMP, Munnich M, Plattner G-K (2013) Spatiotemporal variability and long-term trends of ocean acidification in the California Current System. Biogeosciences 10:193–216

Hedges JI, Stern JH (1984) Carbon and nitrogen determinations of carbonate-containing solids. Limnol Ocean 29:657–663

Hettinger A, Sanford E, Hill TM, Lenz EA, Russell AD, Gaylord B (2013) Larval carry-over effects from ocean acidification persist in the natural environment. Glob Change Biol

Hettinger A, Sanford E, Hill TM, Russell AD, Sato KNS, Hoey J, Forsch M, Page HN, Gaylord B (2012) Persistent carry-over effects of planktonic exposure to ocean acidification in the Olympia oyster. Ecology 93:2758–2768

Hickey BM, Banas NS (2003) Oceanography of the U.S. Pacific Northwest Coastal Ocean and estuaries with application to coastal ecology. Estuaries 26:1010–1031

Hill JK, Wheeler PA (2002) Organic carbon and nitrogen in the northern California current system: comparison of offshore, river plume, and coastally upwelled waters. Prog Ocean 53:369–387

His E, Maurer D (1988) Shell growth and gross biochemical composition of oyster larvae (Crassostrea gigas) in the field. Aquaculture 69:185–194

His E, Robert R, Dinet A (1989) Combined effects of temperature and salinity on fed and starved larvae of the mediterranean mussel Mytilus galloprovincialis and the Japanese oyster Crassostrea gigas. Mar Biol 100:455–463

Hoegh-Guldberg O, Manahan D (1995) Coulometric measurement of oxygen consumption during development of marine invertebrate embryos and larvae. J Exp Biol 198:19–30

Hoenisch B, Ridgwell A, Schmidt DN, Thomas E, Gibbs SJ, Sluijs A, Zeebe R, Kump L, Martindale RC, Greene SE, Kiessling W, Ries J, Zachos JC, Royer DL, Barker S, Marchitto TM, Moyer R, Pelejero C, Ziveri P, Foster GL, Williams B (2012) The Geological Record of Ocean Acidification. Science 335:1058–1063

Hofmann GE, Smith JE, Johnson KS, Send U, Levin LA, Micheli F, Paytan A, Price NN, Peterson B, Takeshita Y, Matson PG, Crook ED, Kroeker KJ, Gambi MC, Rivest EB, Frieder CA, Yu PC, Martz TR (2011) High-Frequency Dynamics of Ocean pH: A Multi-Ecosystem Comparison. PLoS ONE 6:e28983

Hunt CW, Salisbury JE, Vandemark D, McGillis W (2011) Contrasting Carbon Dioxide Inputs and Exchange in Three Adjacent New England Estuaries. Estuaries Coasts 34:68–77

Kelly RP, Foley MM, Fisher WS, Feely RA, Halpern BS, Waldbusser GG, Caldwell MR (2011) Mitigating Local Causes of Ocean Acidification with Existing Laws. Science 332:1036–1037

Kennedy V (1996) Biology of Larvae and Spat. In: The Eastern Oyster : Crassostrea virginica. Maryland Sea Grant College, College Park, Maryland, p 371–421

Kniprath E (1981) Ontogeny of the Molluscan Shell Field: a Review. Zool Scr 10:61–79

Kroeker KJ, Kordas RL, Crim R, Hendriks IE, Ramajo L, Singh GS, Duarte CM, Gattuso J-P (2013) Impacts of ocean acidification on marine organisms: quantifying sensitivities and interaction with warming. Glob Change Biol 19:1884–1896

Kroeker KJ, Kordas RL, Crim RN, Singh GG (2010) Meta-analysis reveals negative yet variable effects of ocean acidification on marine organisms. Ecol Lett 13:1419–1434

Kudo M, Kameda J, Saruwatari K, Ozaki N, Okano K, Nagasawa H, Kogure T (2010) Microtexture of larval shell of oyster, Crassostrea nippona: A FIB-TEM study. J Struct Biol 169:1–5

Kurihara H (2008) Effects of CO2-driven ocean acidification on the early developmental stages of invertebrates. Mar Ecol Prog Ser 373:275–284

Lorrain A, Paulet Y-M, Chauvaud L, Dunbar R, Mucciarone D, Fontugne M (2004) δ13C variation in scallop shells: Increasing metabolic carbon contribution with body size? Geochim Cosmochim Acta 68:3509–3519

Lueker TJ, Dickson AG, Keeling CD (2000) Ocean pCO2 calculated from dissolved inorganic carbon, alkalinity, and equations for K1 and K2: validation based on laboratory measurements of CO2 in gas and seawater at equilibrium. Mar Chem 70:105–119

Maeda-Martinez A. (1987) The rates of calcium deposition in shells of molluscan larvae. Comp Biochem Physiol A Physiol 86:21–28

Marin F, Luquet G, Marie B, Medakovic D (2008) Molluscan shell proteins: Primary structure, origin, and evolution. In: Schatten GP (ed) Current Topics in Developmental Biology, Vol 80. Elsevier Academic Press Inc, San Diego, p 209–276

Massapina C, Joaquim S, Matias D, Devauchelle N (1999) Oocyte and embryo quality in Crassostrea gigas (Portuguese strain) during a spawning period in Algarve, South Portugal. Aquat Living Resour 12:327–333

Matias D, Joaquim S, Ramos M, Sobral P, Leitão A (2011) Biochemical compounds' dynamics during larval development of the carpet-shell clam (Linnaeus, 1758): effects of mono-specific diets and starvation. Helgol Mar Res 65:369–379

McConnaughey TA, Burdett J, Whelan JF, Paull CK (1997) Carbon isotopes in biological carbonates: respiration and photosynthesis. Geochim Cosmochim Acta 61:611–622

McConnaughey TA, Gillikin DP (2008) Carbon isotopes in mollusk shell carbonates. Geo-Mar Lett 28:287–299

McCutchan Jr JH, Lewis Jr WM, Kendall C, McGrath CC (2003) Variation in trophic shift for stable isotope ratios of carbon, nitrogen, and sulfur. Oikos 102:378–390

McElhany P, Busch DS (2013) Appropriate pCO(2) treatments in ocean acidification experiments. Mar Biol 160:1807–1812

McFarland K, Donaghy L, Volety A (2013) Effect of acute salinity changes on hemolymph osmolality and clearance rate of the non-native mussel, Perna viridis, and the native oyster, Crassostrea virginica, in Southwest Florida. Aquat Invasions 8:299–310

Mehrbach, C C, C.H. (1973) Measurement of the apparent dissociation constants of carbonic acid in seawater at atmospheric pressure. Limnol Ocean 18:897–907

Melzner F, Stange P, Trübenbach K, Thomsen J, Casties I, Panknin U, Gorb SN, Gutowska MA (2011) Food Supply and Seawater pCO2 Impact Calcification and Internal Shell Dissolution in the Blue Mussel Mytilus edulis. PloS One 6

Metcalfe NB, Monaghan P (2001) Compensation for a bad start: grow now, pay later? Trends Ecol Evol 16:254–260

Moran AL, Manahan DT (2004) Physiological recovery from prolonged starvation'in larvae of the Pacific oyster Crassostrea gigas. J Exp Mar Biol Ecol 306:17–36

Moran AL, McAlister JS (2009) Egg Size as a Life History Character of Marine Invertebrates: Is It All It's Cracked Up to Be? Biol Bull 216:226–242

Mucci A (1983) The solubility of calcite and aragonite in seawater at various salinities, temperatures, and one atmosphere total pressure. Am J Sci 283:780–799

Muranaka M, Lannan J (1984) Broodstock Management of Crassostrea-Gigas - Environmental-Influences on Broodstock Conditioning. Aquaculture 39:217–228

Norris RD, Turner SK, Hull PM, Ridgwell A (2013) Marine Ecosystem Responses to Cenozoic Global Change. Science 341:492–498

Owen EF, Wanamaker Jr AD, Feindel SC, Schöne BR, Rawson PD (2008) Stable carbon and oxygen isotope fractionation in bivalve (Placopecten magellanicus) larval aragonite. Geochim Cosmochim Acta 72:4687–4698

Parker LM, Ross PM, O'Connor WA, Borysko L, Raftos DA, Pörtner H (2012) Adult exposure influences offspring response to ocean acidification in oysters. Glob Change Biol 18:82–92

Parker L, Ross P, O'Connor W, Pörtner H, Scanes E, Wright J (2013) Predicting the Response of Molluscs to the Impact of Ocean Acidification. Biology 2:651–692

Pechenik JA (2006) Larval experience and latent effects—metamorphosis is not a new beginning. Integr Comp Biol 46:323–333

Richmond CE, Woodin SA (1996) Short-term fluctuations in salinity: Effects on planktonic invertebrate larvae. Mar Ecol Prog Ser 133:167–177

Ries JB (2011) Skeletal mineralogy in a high-CO_2 world. J Exp Mar Biol Ecol 403:54–64

Ries JB, Cohen AL, McCorkle DC (2009) Marine calcifiers exhibit mixed responses to CO_2-induced ocean acidification. Geology 37:1131–1134

Romanek CS, Grossman EL, Morse JW (1992) Carbon isotopic fractionation in synthetic aragonite and calcite: effects of temperature and precipitation rate. Geochim Cosmochim Acta 56:419–430

Talmage SC, Gobler CJ (2009) The effects of elevated carbon dioxide concentrations on the metamorphosis, size, and survival of larval hard clams (Mercenaria

mercenaria), bay scallops (Argopecten irradians), and Eastern oysters (Crassostrea virginica). Limnol Ocean 54:2072–2080

Talmage SC, Gobler CJ (2011) Effects of Elevated Temperature and Carbon Dioxide on the Growth and Survival of Larvae and Juveniles of Three Species of Northwest Atlantic Bivalves. PLoS One 6

Tang B, Liu B, Wang G, Zhang T, Xiang J (2006) Effects of various algal diets and starvation on larval growth and survival of Meretrix meretrix. Aquaculture 254:526–533

Uriarte I, Farias A, Hernandez J, Schafer C, Sorgeloos P (2004) Reproductive conditioning of Chilean scallop (Argopecten purpuratus) and the Pacific oyster (Crassostrea gigas): effects of enriched diets. Aquaculture 230:349–357

Vargas CA, Hoz M de la, Aguilera V, San Martin V, Manriquez PH, Navarro JM, Torres R, Lardies MA, Lagos NA (2013) CO2-driven ocean acidification reduces larval feeding efficiency and changes food selectivity in the mollusk Concholepas concholepas. J Plankton Res 35:1059–1068

Verardo DJ, Froelich PN, McIntyre A (1990) Determination of organic carbon and nitrogen in marine sediments using the Carlo Erba NA-1500 Analyzer. Deep Sea Res Part Ocean Res Pap 37:157–165

Waldbusser GG, Bergschneider H, Green MA (2010) Size-dependent pH effect on calcification in post-larval hard clam Mercenaria spp. Mar Ecol Prog Ser 417:171–182

Waldbusser GG, Salisbury JE (2014) Ocean Acidification in the Coastal Zone from an Organism's Perspective: Multiple System Parameters, Frequency Domains, and Habitats. Annu Rev Mar Sci 6

Waldbusser GG, Brunner EL, Haley BA, Hales B, Langdon CJ, Prahl FG (2013) A developmental and energetic basis linking larval oyster shell formation to acidification sensitivity. Geophys Res Lett 40:2171–2176

Waldbusser GG, Voigt EP, Bergschneider H, Green MA, Newell RIE (2011) Biocalcification in the eastern oyster (Crassostrea virginica) in relation to long-term trends in Chesapeake Bay pH. Estuaries Coasts 34:221–231

Walker BD, McCarthy MD (2012) Elemental and isotopic characterization of dissolved and particulate organic matter in a unique California upwelling system: Importance of size and composition in the export of labile material. Limnol Ocean 57:1757–1774

Waller TR (1981) Functional morphology and development of veliger larvae of the European oyster. Smithson Contrib Zool 328:1–70

Weiss IM, Tuross N, Addadi L, Weiner S (2002) Mollusc larval shell formation: amorphous calcium carbonate is a precursor phase for aragonite. J Exp Zool 293:478–491

White MM, McCorkle DC, Mullineaux LS, Cohen AL (2013) Early Exposure of Bay Scallops (Argopecten irradians) to High CO2 Causes a Decrease in Larval Shell Growth. PLoS ONE 8

Whiting MC, McIntire CD (1985) An Investigation of Distributional Patterns in the Diatom Flora of Netarts Bay, Oregon, by Correspondence Analysis. J Phycol 21:655–661

Yokoo N, Suzuki M, Saruwatari K, Aoki H, Watanabe K, Nagasawa H, Kogure T (2011) Microstructures of the larval shell of a pearl oyster, Pinctada fucata, investigated by FIB-TEM technique. Am Miner 96:1020–1027

APPENDICES

Appendix 1: Fraction Metabolic Carbon in D-hinge Shell

The objective of these additional experiments was to further investigate the incorporation of ambient DIC carbon (versus metabolic carbon, reviewed by McConnaughey and Gillikin, 2008) into D-hinge shell, by exposing D-hinge larvae to a range of different carbonate chemistry conditions, with independently varying PCO_2 and Ω_{arag} (Table 5). The objective was to test if the low incorporation of metabolic carbon in early shell observed in cohorts at WCH is conserved among all larvae regardless of the level of acidification stress. In the main body of this thesis, I followed how the incorporation of ambient DIC carbon into shell changes with age in three different cohorts of larvae: one that experienced low PCO_2 and a moderately Ω_{arag}; one that experienced a high PCO_2 and a moderately low omega; and one that experienced low PCO_2 and a high Ω_{arag} (Table 2, Fig.1). With this experiment, I hoped to further explore which carbonate chemistry parameters are responsible for driving the incorporation of ambient DIC carbon into early larval shell, by taking advantage of the unique carbonate chemistry manipulation technique developed by Waldbusser et al., (in prep). In order to make the experiment logistically feasible, I focused on the formation of the D-hinge shell (0-48 hours after fertilization), which has been identified as particularly vulnerable life-stage (reviewed by Gazeau et al., 2013) and a period when the precipitation of shell depends most heavily on ambient carbonate chemistry (Waldbusser et al., 2013, Fig. 4).

Calculating the fraction of metabolic carbon in the larval shell requires being able to measure $\delta^{13}C$ of (1) the ambient seawater DIC, (2) the larval tissue, and (3) the larval shell carbonate. At WCH, the cohorts were large enough that sample mass was not limiting for these measurements (primary sample mass was $0.5 - 2$ g), but with the these carbonate chemistry manipulation experiments, I was limited by the 500 mL volume of our incubation containers, which was stocked with no more than 5000 larvae to avoid container effects. At 48 hours, the larvae are less than 200 ng dry weight each, small enough that 30,000 larvae (6 mg dry weight) are needed in order to make one measurement of $\delta^{13}C$ of tissue. In order to estimate the tissue value, I made the assumption that the egg $\delta^{13}C$ value is representative of the larval tissue during the first 48 hours. Fig. 3 shows that in the WCH cohorts, the organic carbon $\delta^{13}C$ stays roughly level

until the larvae start feeding (at one or two days depending on when they were first given algae), giving me confidence to make this assumption. Note that the number presented in the Table 1 is assumed from other egg values observed from MBP oysters (not presented) as the egg sample was not run for this particular experiment.

The next challenge was to measure the $\delta^{13}C$ of the shell carbon on very small amounts of shell carbonate. Even with the shell material of all 5000 larvae, I was nearing the analytical limit of the CEOAS Stable Isotope Laboratory. In order to retain all the larvae with the minimum loss, I passed the water containing the larvae from each experimental container over pre-combusted glass fiber filters (GF/F), rinsed the filters with the captured larvae with DI water, and dried them at less than 45°C for storage. I modified the usual carbonate measuring protocol used by CEOAS Stable Isotope Laboratory by directly introducing pieces (~ 7mm diameter) of the filters into the glass vials of the Kiel III, by increasing the volume of phosphoric acid added to each vial, and by increasing the reaction time to allow the acid to penetrate all the filter pieces. DIC $\delta^{13}C$ was measured by the same methods described in the main text. From these data, I computed an integrated fraction metabolic carbon in larval shell for each of the replicate samples. The isotope data and the carbonate chemistry conditions for each treatment are presented in Table 5. Some uncertainties remain as to the success of these modifications, so interpretations of these data are not presented. The primary source of uncertainty in these calculations is in the measurement of $\delta^{13}C$ of the shell carbonate. To follow up on these data, I ran a second experiment with a larger suite of treatment conditions. However, due to more uncertainties with the analytical technique for measuring the shell carbonate $\delta^{13}C$ and the health of the larvae in this experiment, these data are not presented here.

Table 5. Results of the fraction metabolic carbon in D-hinge shell experiment.

	Carbonate Chemistry Conditions						Fraction Metabolic Carbon	$\delta^{13}C$		
	Talk (µeq kg^{-1})	DIC (µM kg^{-1})	PCO2 (µatm)	pH$_{sws}$	$\Omega_{calcite}$	Ω_{arag}		egg	DIC	shell
White (1)	1605	1360	240	8.09	3.89	2.17	0.118	-20	-1.58	-1.05
White (2)	1605	1360	240	8.09	3.89	2.17	0.133	-20	-1.74	-1.46
White (3)	1605	1360	240	8.09	3.89	2.17	0.126	-20	-1.72	-1.32
Blue (1)	2138	1746	207	8.24	6.73	3.75	0.114	-20	-2.21	-1.54
Blue (2)	2138	1746	207	8.24	6.73	3.75	0.116	-20	-2.42	-1.75
Blue (3)	2138	1746	207	8.24	6.73	3.75	0.115	-20	-2.44	-1.76
Green (1)	1308	1151	292	7.94	2.38	1.32	0.11	-20	-1.48	-0.81
Green (2)	1308	1151	292	7.94	2.38	1.32	0.12	-20	-1.37	-0.9
Green (3)	1308	1151	292	7.94	2.38	1.32	0.127	-20	-1.37	-1.03
Red (1)	2066	1935	804	7.74	2.62	1.46	0.099	-20	-2.07	-1.15
Red (2)	2066	1935	804	7.74	2.62	1.46	0.079	-20	-2.11	-0.81
Red (3)	2066	1935	804	7.74	2.62	1.46	0.104	-20	-2.01	-1.17
Yellow (1)	3459	3148	863	7.91	6.43	3.59	0.094	-20	-2.30	-1.26
Yellow (2)	3459	3148	863	7.91	6.43	3.59	0.11	-20	-2.15	-1.41
Yellow (3)	3459	3148	863	7.91	6.43	3.59	0.091	-20	-2.29	-1.21
Control (1)	2262	2151	1087	7.66	2.48	1.38	0.116	-20	-0.18	0.23
Control (2)	2262	2151	1087	7.66	2.48	1.38	0.119	-20	-0.15	0.19
Control (3)	2262	2151	1087	7.66	2.48	1.38	0.125	-20	-0.08	0.13
Control (4)	2262	2151	1087	7.66	2.48	1.38	0.1	-20	0.70	1.33
Control (5)	2262	2151	1087	7.66	2.48	1.38	0.101	-20	0.70	1.32
Control (6)	2262	2151	1087	7.66	2.48	1.38	0.089	-20	0.53	1.39

Gazeau F, Parker LM, Comeau S, Gattuso J-P, O'Connor WA, Martin S, Poertner H-O, Ross PM (2013) Impacts of ocean acidification on marine shelled molluscs. Mar Biol 160:2207–2245

McConnaughey TA, Gillikin DP (2008) Carbon isotopes in mollusk shell carbonates. Geo-Mar Lett 28:287–299

Waldbusser, G.G., Hales, B., Langdon, C.J., Haley, B.A., Brunner, E.L., Gray, M. ((in prep)) Acute effects of carbonate system parameters on prodissoconch I development and growth in larval bivalves.

Appendix 2: Oxygen Isotopes in Shell and Water

Both carbon and oxygen isotopes in biogenic carbonates contain information about ambient environmental conditions; the oxygen isotopes from foraminifera calcite ($\delta^{18}O$) are commonly used a paleoproxy for ocean temperature and ice volume (Shackleton, 1987; Zachos et al., 2001), while carbon isotopes are used to gain insight into ocean productivity, upwelling, and to trace anthropogenic carbon (Steens et al., 1992; Schmittner et al., 2013). Metabolic carbon in shell can bias the DIC $\delta^{13}C$ signal and stand in the way of accurately reconstructing past DIC $\delta^{13}C$ from mollusk shell carbonates. Therefore, much of the work done to understand the contribution of metabolic carbon to calcification has been from the perspective of trying to predict and correct for these "vital effects" (McConnaughey and Gillikin, 2008).

Isotopic fractionation between the ambient seawater and biogenic carbonates can be kinetic (McConnaughey, 2003), as is common in non-photosynthetic corals (McConnaughey 1989). Mollusks, in general, do not show kinetic isotope effects, which is likely due relatively mild alkalization at the sites of calcification, and to the use of the enzyme carbonic anhydrase, which catalyzes the hydroxylation of CO_2, thereby reducing the fractionation in that reaction (McConnaughey and Gillikin, 2008). Our larval shells do not show evidence of kinetic isotope effects, which would manifest themselves in strong positive correlation between $\delta^{13}C$ and $\delta^{18}O$ in carbonates (Figure 6). Therefore, I am confident in calculating the fraction of metabolic carbon in larval shell using the model of McConnnaughey (1997), which assumes an equilibrium fractionation between bicarbonate and aragonite. There are other caveats to that model, however (McConnaughey and Gillikin, 2008). First, it assumes no fractionation between tissue carbon and metabolic CO_2, although it is likely that *haemolymph* DIC would have the ^{13}C concentrated in HCO_3^- and ^{12}C concentrated in the CO_2, resulting in a metabolic carbon pool that is lighter than the overall haemolymph DIC. Second, it does not specify the speciation of DIC, although it is known that in seawater carbon isotopes are partitioned into the dissolved species predictably based on the pH (Zeebe and Wolf-Gladrow, 2001). To address the second concern, I calculated the fraction metabolic carbon in each shell sample using the ambient HCO_3^- $\delta^{13}C$ (calculated) instead of the measured DIC $\delta^{13}C$, and

found no difference in the patterns that are presented in Figure 5. In the absence of dependable information about these two processes in our larvae, the fraction metabolic carbon is presented as calculated from the simple model of McConnaughey (1997).

There is a pronounced lightening of the oxygen isotopes (-2 ‰) in the middle of the larval period in May (Table 6) that coincides with a period of lower salinity in Netarts Bay and in the larval incubation tanks (Table 2). Oregon's coastal rivers are generally depleted in ^{18}O compared to seawater (Kendall and Coplan, 2001), so this is the pattern that would be expected based on the low salinity values for this period. It is also possible that the reason the salinity dropped so dramatically in Netarts Bay in May 2011 was because the Columbia River plume was forced south alongside the shore due to a unusual combination of hydrographic and oceanographic factors (Hales, unpublished).

$\delta^{18}O$ *Measurement Methods*

Larval shell $\delta^{18}O$ was measured in the same analytical step as $\delta^{13}C$, by reacting 19-50 freeze-dried larvae with ~105% orthophosphoric acid at 70°C for 5 minutes in a Finnigan Keil III device, and measuring the isotopic signal of the resulting CO_2 on a MAT 252 mass spectrometer by dual inlet mass spectrometry. Accuracy was better than 0.14‰, and repeatability was 0.06‰. Water $\delta^{18}O$ was measured following a modification of the method by Epstein and Mayeda, (1953), also at OSU's CEOAS Stable Isotope Laboratory. Water samples were first pipetted into glass bottles, and allowed to equilibrate to 18°C. The headspace was flushed with He, refilled with CO_2 gas, and allowed to come to isotopic equilibration with the water for 12 hours. Then the oxygen isotopes of the water are analyzed by dual inlet mass spectrometry using the DeltaPlus XL. Accuracy was better than 0.04‰, and repeatability was 0.01‰.

Table 6. Oxygen isotopes of shell carbonates and tank incubation water

Age (days)	May water $\delta^{18}O$ V-SMOW	May shell $\delta^{18}O$ VPDB	August water $\delta^{18}O$ V-SMOW	August shell $\delta^{18}O$ VPDB	August (trt) water $\delta^{18}O$ V-SMOW	August (trt) shell $\delta^{18}O$ VPDB
0	-	-	**-0.34**	-	-0.36	-
1	-	-	**-0.34**	**-0.81**	-0.28	-0.84
2	-1.35	**-3.05**		**-**	-	-
3	-	-	-0.30	**-1.04**	-0.33	-1.05
5	-1.37	-2.64	-0.28	**-0.90**	-0.28	-0.89
7	-	-	-0.22	**-0.89**	-0.21	-0.86
8	-3.42	**-2.58**	-	-	-	-
9	-	-	-0.42	-0.82	-0.44	-0.95
11	-3.41	-2.96	-1.14	-0.97	-1.17	-0.92
13	-3.96	-3.17	-0.53	-1.18	-0.47	-1.07
15	-3.95	-3.32	-0.40	-1.00	-0.33	-0.96
17	-3.14	**-3.51**	-0.40	-1.02	-0.40	-0.99
19	-	-3.76	-0.41	-0.94	-0.38	-0.90
21	-	-	-	-1.03	-	-0.92

Bolded values are average of two replicate measurements

Figure 6. Coherence of δ¹³C and δ¹⁸O in larval shell carbonates. There is no evidence of kinetic isotope effects, which would manifest in a strong positive relationship between shell δ¹³C and shell δ¹⁸O.
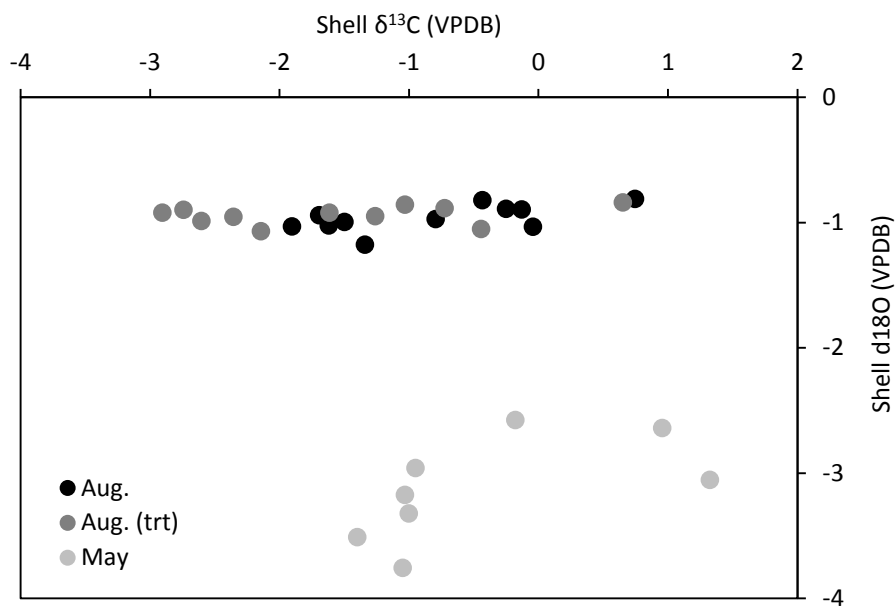
Epstein S, Mayeda T (1953) Variation of O18 content of waters from natural sources. Geochim Cosmochim Acta 4:213–224

Kendall C, Coplen TB (2001) Distribution of oxygen-18 and deuterium in river waters across the United States. Hydrol Process 15:1363–1393

McConnaughey T (1989) 13C and 18O isotopic disequilibrium in biological carbonates: II. In vitro simulation of kinetic isotope effects. Geochim Cosmochim Acta 53:163–171

McConnaughey TA (2003) Sub-equilibrium oxygen-18 and carbon-13 levels in biological carbonates: carbonate and kinetic models. Coral Reefs 22:316–327

McConnaughey TA, Burdett J, Whelan JF, Paull CK (1997) Carbon isotopes in biological carbonates: respiration and photosynthesis. Geochim Cosmochim Acta 61:611–622

McConnaughey TA, Gillikin DP (2008) Carbon isotopes in mollusk shell carbonates. Geo-Mar Lett 28:287–299

Schmittner A, Gruber N, Mix AC, Key RM, Tagliabue A, Westberry TK (2013) Biology and air–sea gas exchange controls on the distribution of carbon isotope ratios (δ13C) in the ocean. Biogeosciences 10:5793–5816

Shackleton NJ (1987) Oxygen isotopes, ice volume and sea level. Quat Sci Rev 6:183–190

Steens TNF, Ganssen G, Kroon D (1992) Oxygen and carbon isotopes in planktonic foraminifera as indicators of upwelling intensity and upwelling-induced high productivity in sediments from the northwestern Arabian Sea. Geol Soc Lond Spec Publ 64:107–119

Zachos J, Pagani M, Sloan L, Thomas E, Billups K (2001) Trends, Rhythms, and Aberrations in Global Climate 65 Ma to Present. Science 292:686–693

Zeebe R, Wolf-Gladrow D (2001) Stable isotope fractionation. In: Zeebe R, Wolf-Gladrow D (eds) Elsevier Oceanography Series. Elsevier, p 141–250

Appendix 3: Dissolvability of D-hinge Shell Microstructure

There appear to be structural differences between the earliest laid down shell (sometimes called Prodissoconch I) and the carbonate laid down later in the larval period (called Prodissoconch II). Three distinct microstructures of larval shell have been previously described in different genera of bivalve (Carriker et al. 1979, Waller, 1981, Weiss et al., 2002), and I observed these same microstructures in our samples (Figure 7). The "outer prismatic layer" corresponds to the initial shell, which is laid down between 12 and 17 hours post fertilization in *Crassostrea gigas* at 25 °C. Recent TEM imaging of FIB-prepared larval shells have shown differences in crystalline structure among the three layers (Kudo et al., 2010; Yokoo et al., 2011).

This experiment investigated differences in the dissolvability of these different parts of the larval shell by exposing whole shells to different strengths of mineral acid. I exposed 10 mg sub-samples of 3 day old freeze-dried larvae from the August unbuffered cohort to 10 concentrations of HNO_3 ranging from 0 (DI water) to 1 M for ~15 minutes, rinsed them 3 times with DI, dried them overnight, and then imaged with SEM to look at patterns of dissolution. The partially-dissolved larvae were mounted on double-sided carbon tape, coated with an Au-Pd mixture, and imaged on a FEI Quanta 600F environmental SEM. Images of selected treatments are shown in Figure 8. From these images, it is apparent that the D-hinge shell is more dissolvable than the later larval shell; with increasing acid concentration, the D-hinge shell is first preferentially pitted, and then preferentially dissolved.

It is assumed that all the microstructures present are composed of aragonite (Kudo et al., 2010l; Yokoo et al., 2011), with relatively low Mg concentrations (Waldbusser et al., unpublished), so their thermodynamic solubility should be roughly the same. It is known that microstructure and crystalline surface area are sometimes more important than polymorph for determining the rate of dissolution of biogenic carbonates (Kidwell and Grover, 2005), and as such, there are several possible non-thermodynamic explanations for this observation. First, it is possible that the periostracum overlying the initial shell is weaker or more porous than the later periostracum, and the acid may have therefore had more contact with the initial shell than the parts of the shell that were better

protected. A second explanation is that the arrangement of crystals within the microstructure itself could make it susceptible to more rapid dissolution. Based on the diffraction pattern of the initial shell and preponderance of twins, both Kudo et al., (2010) and Yokoo et al., (2011) suggest that the initial shell is precipitated more rapidly than later shell. The same structural mechanism that allows for the initial rapid precipitation could mean that the initial shell has crystals with more surface area vulnerable to attack from the acid. More work is needed to further investigate the mechanical properties of the initial shell, explore what they can tell us about the susceptibility of larvae to changes in ambient carbonate chemistry during the initial shell formation period.
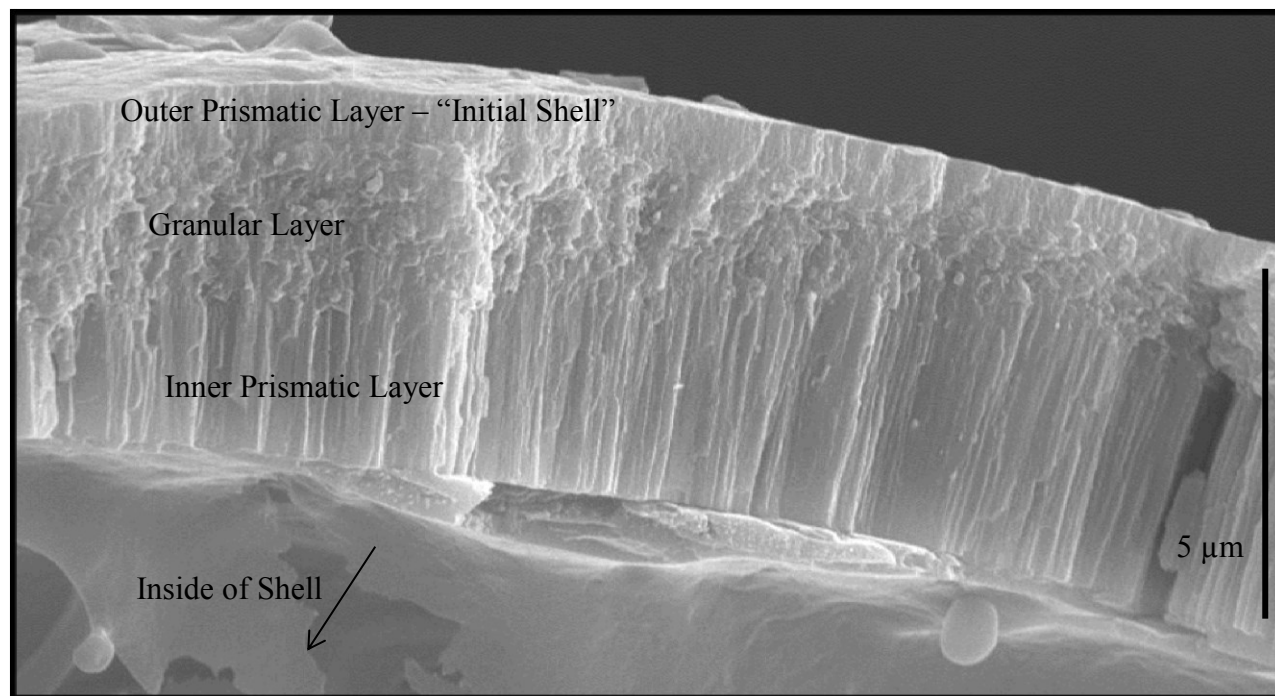
Figure 7. SEM image of a fractured cross-section of at 13 day old *Crassostrea gigas* larva from the May cohort. The cross-section is from a part of the shell underlying the Prodissoconch I shell.
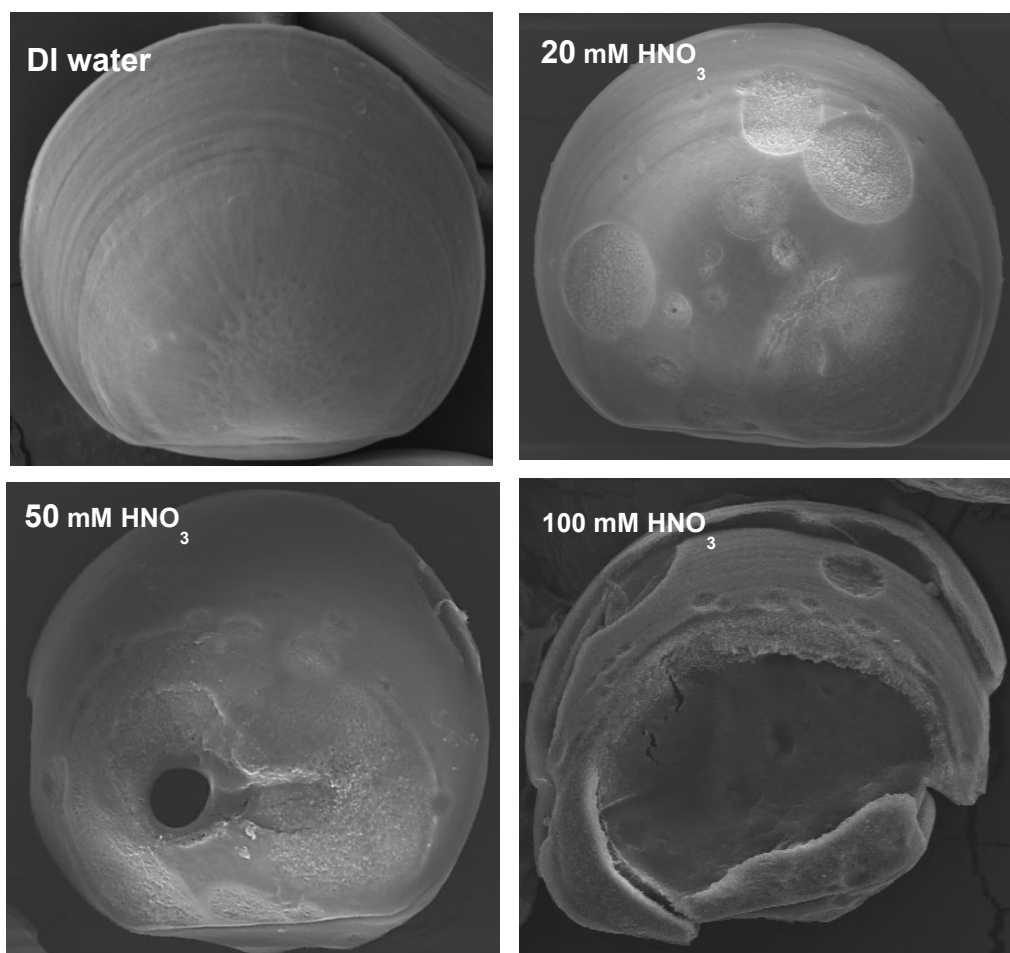
Figure 8. SEM images of 3 day old August unbuffered larvae exposed to different concentrations of HNO$_3$. With increasing acid concentration, the D-hinge shell is first preferentially pitted, and then preferentially dissolved.

Carriker MR, Palmer RE, Oceanic USN, Grant AAO of S, Programs E (1979) Ultrastructural morphogenesis of prodissoconch and early dissoconch valves of the oyster Crassostrea virginica. College of Marine Studies, University of Delaware

Kudo M, Kameda J, Saruwatari K, Ozaki N, Okano K, Nagasawa H, Kogure T (2010) Microtexture of larval shell of oyster, Crassostrea nippona: A FIB-TEM study. J Struct Biol 169:1–5

Waller TR (1981) Functional morphology and development of veliger larvae of the European oyster. Smithson Contrib Zool 328:1–70

Weiss IM, Tuross N, Addadi L, Weiner S (2002) Mollusc larval shell formation: amorphous calcium carbonate is a precursor phase for aragonite. J Exp Zool 293:478–491

Yokoo N, Suzuki M, Saruwatari K, Aoki H, Watanabe K, Nagasawa H, Kogure T (2011) Microstructures of the larval shell of a pearl oyster, Pinctada fucata, investigated by FIB-TEM technique. Am Miner 96:1020–1027